

1 **Attribution of high resolution streamflow trends in Western**
2 **Austria – an approach based on climate and discharge**
3 **station data**

4
5 **C. Kormann¹, T. Francke¹, M. Renner² and A. Bronstert¹**

6 [1]{Institute of Earth and Environmental Science, University of Potsdam, Potsdam, Germany}

7 [2]{Biospheric Theory and Modeling, Max Planck Institute for Biogeochemistry, Jena,
8 Germany}

9 Correspondence to: C. Kormann (ckormann@uni-potsdam.de)

10

11 **Abstract**

12 The results of streamflow trend studies are often characterised by mostly insignificant trends and
13 inexplicable spatial patterns. In our study region, Western Austria, this applies especially for
14 trends of annually averaged runoff. However, analysing the altitudinal aspect, we found that
15 there is a trend gradient from higher-altitude to lower-altitude stations, i.e. a pattern of mostly
16 positive annual trends at higher stations and negative ones at lower stations. At mid-altitudes, the
17 trends are mostly insignificant. Here we hypothesize that the streamflow trends are caused by the
18 following two main processes: On the one hand, melting glaciers produce excess runoff at
19 higher-altitude watersheds. On the other hand, rising temperatures potentially alter hydrological
20 conditions in terms of less snowfall, higher infiltration, enhanced evapotranspiration etc., which
21 in turn results in decreasing streamflow trends at lower-altitude watersheds. However, these
22 patterns are masked at mid-altitudes because the resulting positive and negative trends balance
23 each other. To support these hypotheses, we attempted to attribute the detected trends to specific
24 causes. For this purpose, we analysed the trends on a daily basis, as the causes for these changes
25 might be restricted to a smaller temporal scale than the annual one. This allowed for the explicit
26 determination of the exact days of year (DOY) when certain streamflow trends emerge, which
27 were then linked with the corresponding DOYs of the trends and characteristic dates of other

1 observed variables, e.g. the average DOY when temperature crosses the freezing point in spring.
2 Based on these analyses, an empirical statistical model was derived that was able to simulate
3 daily streamflow trends sufficiently well. The identified explanatory variables were the minimum
4 temperature, the first derivative of the mean annual hydrograph indicating rising or falling
5 conditions and the glacier percentage in the watershed. Analyses of subdaily streamflow changes
6 provided additional insights. Finally, the present study supports many modelling approaches in
7 the literature who found out that the main drivers of alpine streamflow changes are increased
8 glacial melt, earlier snow melt and lower snow accumulation in wintertime. However, further
9 research is needed to explicitly determine which processes related to positive temperature trends
10 lead to the summertime streamflow decreases.

11

12 **Keywords:** Trend attribution; Trend detection; Mountain hydrology; Streamflow; Climate
13 Change

14

15 **1. Introduction**

16 Climate change alters the hydrological conditions in many regions (Parry et al., 2007). Especially
17 watersheds in mountain regions are more sensitive compared to those in lowlands (Barnett et al.,
18 2005, Viviroli et al., 2011). This is mostly due to the strong connection between mountain
19 hydroclimatology and temperature increase, which is at least twice as strong in mountainous
20 areas compared to the global average (Brunetti et al., 2009): On the one hand, increasing
21 temperatures result in diminishing glaciers, earlier snowmelt and less precipitation falling in the
22 form of snow; on the other hand, the local climate is changed by interdependencies like e.g. the
23 snow-albedo feedback (Hall et al., 2008).

24 A multitude of studies have tried to assess the detailed impacts of these changes through
25 modeling approaches, especially for future scenarios (e.g. Magnusson et al., 2010, Tecklenburg
26 et al., 2012, Vormoor et al., 2014). Another way of understanding climate change impacts on
27 local hydrology is to analyse trends in observed streamflow data (e.g. Stahl et al., 2010, Dai et
28 al., 2009). However, the aim of finding clear changing patterns is often hindered by strong noise
29 in the data, as well as the fact that signals are usually small. Viviroli et al., 2011 note in their

1 review paper on climate change and mountain water resources, that trend studies in alpine
2 regions often report “*inconclusive or misleading findings*”.

3 However, other studies with different statistical approaches to analyse streamflow changes in
4 alpine regions were published: In the mountainous areas of western North America, many studies
5 agree that snowmelt and thus spring freshet is appearing earlier in the year (e.g. Stewart et al.,
6 2005, Mote et al., 2005; Knowles et al., 2006). However, most of these studies are based on
7 trends of indicators like ‘centre of volume’ or ‘day of occurrence of the annual peak flow’, which
8 serve as proxies to indicate consequences of global warming on alpine streamflow (i.e. earlier
9 snowmelt). The application of these measures is problematic: Whitfield (2013) claims that the
10 ‘centre of volume’ is affected by other factors than temperature alone and has several
11 shortcomings. Déry et al. (2009) found out that these metrics should be avoided, because they are
12 sensitive to factors such as record length, streamflow seasonality and data variability. Contrary to
13 these indicators, a measure that is based on a harmonic filter (Renner and Bernhofer, 2011)
14 provides more robust estimates of the timing of the hydrological cycle. Other studies analysed
15 temporally highly-resolved trends (Kim and Jain, 2010, Déry et al., 2009, Kormann et al., 2014).
16 These trends in daily resolution have the advantage, that not only a shift in snowmelt timing but
17 also other increases or decreases of the streamflow volume are revealed (Déry et al., 2009).
18 Furthermore, a more detailed picture of the changes can be obtained by daily trends than by
19 seasonal or annual averages, where a lot of the information is lost by averaging data over a
20 certain period of time. In addition, the timing of daily trends (i.e. the day of year when a trend
21 turns up) reveals supplementary information on potential drivers of streamflow trends (Kormann
22 et al., 2014).

23 In hydroclimatology, the proof that observed changes are significantly different from variations
24 that could be explained by natural variability is referred to as *trend detection*, whereas *trend*
25 *attribution* describes the assignment of these changes to specific causes. Kundzewicz (2004)
26 underlines the importance of not only trend detection but also trend attribution to understand the
27 reasons for these changes. In this context, it is common practice to set up comparisons or
28 correlations between the variable under consideration and the features of the system in which it
29 is embedded (Merz et al., 2012a). However, previous analyses usually often considered trend
30 magnitudes as the main subject of investigation, e.g. the correlation of observed streamflow trend

1 magnitudes with certain catchment characteristics (e.g. glacier coverage). In addition, trends
2 used for correlation analyses were mainly derived from annual or seasonal (3-monthly)
3 streamflow averages. Both of these approaches are only partially capable of attributing trends, as
4 streamflow integrates multiple processes across the watershed and different time scales. Hence
5 the isolation of trends, that are caused by one single source, is often not possible, resulting in
6 ambiguous outcomes (Merz et al., 2012a). Additionally, correlation can only give hints and does
7 not imply causation. This is especially true in our case, as many of the watershed attributes are
8 themselves correlated with each other (the higher a watershed, the more glaciated and the less
9 vegetated it usually is).

10 In recent years, there has been some progress towards the attribution of streamflow trends via
11 other approaches: Bard et al. (2011) made a relevant step forward by regime-specific trend
12 analyses, as trend causing processes differ from one regime to another. Déry et al. (2009) used a
13 simple model to simulate the cause-and-effect relations between the volume/timing of snowmelt
14 and streamflow. Stewart et al. (2008) reviewed snowmelt-induced streamflow changes in the
15 literature and came to the conclusion, that especially at lower elevations, declining snowpacks
16 and less snowfall affect streamflow quantities.

17 Apart from the hydrological changes caused by earlier spring snowmelt, it is often difficult to
18 find robust links between trend causes and their effects in observational data. Few studies have
19 analysed the long-term effects of glacier mass loss on streamflow. Glaciers may have already
20 reached the turning point when glacier mass has decreased to such a degree that meltwater
21 volumes are reduced as well (Braun et al., 2000). Stahl and Moore (2006) fitted a regression
22 model for August streamflow and then analysed trends in the residuals. The regression model
23 accounted for the climate controls, so if the trends in the residuals were negative, they were
24 attributed to increasing glacier melt. They found that most of the glacier fed streams are in the
25 state of decreasing meltwater volumes. In Europe, however, Pellicciotti et al. (2010) related ice
26 volume changes with streamflow trends and showed that streamflow is still increasing in four
27 Swiss watersheds with high glacier coverage, and decreasing in one watershed with low
28 coverage.

29 Next to changes through earlier snowmelt and increased glacial melt, climate change also
30 influences streamflow through e.g. increasing evapotranspiration (ET) (Walter et al., 2004) or an

1 increase of the timber line (Walther, 2003). However, robust links between detected trends and
2 their causes are missing.

3 Summing up, there are several studies that elaborate on certain aspects of trend causes in alpine
4 catchments. Hence, an integrated attempt would be desirable. For this purpose, the present study
5 combines the benefits of a temporally highly resolved trend analysis that is applicable to all
6 different alpine runoff regimes with hydrological process understanding to explain seasonal
7 streamflow changes in Western Austria. We aim to extend the knowledge about regional trend
8 causes, with the attempt to provide a holistic picture of the changes found under different alpine
9 streamflow conditions. We limit our study to changes in mean values, and exclude analyses of
10 extreme values since these changes might be caused by different processes. For further reading
11 on low flow and flood regime changes, see e.g. Birsan et al. (2005), Parajka et al. (2009), Parajka
12 et al. (2010), Blöschl et al. (2011), Hall et al. (2014).

13 Our study is divided in two parts, (1) an analysis of annually averaged trends/indicators and
14 (2) an analysis of seasonally highly resolved trends. On the basis of the findings in the first part,
15 we derived the following hypotheses:

- 16 • In higher-altitude, glaciated watersheds in the study region, rising temperatures result in
17 increased glacial melt, which in turn cause positive annual streamflow trends. Most of the
18 larger glaciers still have not reached the point where annual streamflow decreases
19 because of decreasing glacier area.
- 20 • In lower-altitude, unglaciated watersheds, increasing temperatures result in earlier
21 snowmelt and less precipitation falling as snow. This in turn leads to multiple
22 hydrological changes such as higher evapotranspiration, higher infiltration or changing
23 storage characteristics, to name a few. The negative streamflow trends in the study region
24 are a result of these changes.
- 25 • In watersheds located at middle altitudes and covered by a smaller glacier percentage,
26 both processes are prevalent to a lesser degree and compensate for each other.

27 To support these theories, it is necessary to attribute the streamflow trends. This is done in the
28 second part of the present study: It is realised via a seasonal examination of the changes, as the
29 driving processes for these changes might be limited to a smaller scale than the annual one.

30

1 **2. Data**

2 The study area is situated in Western Austria, mainly in North Tirol. With 970 ± 290 mm
3 average precipitation amount per year (based on station data, 1980–2010), this is a relatively dry
4 region in the Alps as it is situated in the rain shadow of the northern and southern Alpine border
5 ranges. The study region includes altitudes from 673 m up to 3768 m a.s.l., with an extent of
6 roughly 200 km in the East-West direction and 60 km in the North-South direction. There is a
7 temperate climate with distinct precipitation maxima in summer. The majority of the watersheds
8 under study drain into the Inn, Drava and Lech rivers, all tributaries of the Danube. For the most
9 part, grassland and coniferous forest dominate the landuse in the lower catchment areas, whereas
10 the percentage of rocky areas with little or no vegetation increases with increasing watershed
11 altitude. Due to the strong influence of glacier and snow melt, mostly glacial and nival discharge
12 regimes prevail which means discharge quantities have a distinct seasonal cycle with maxima in
13 spring or summer and low flows in winter.

14 In the present analysis, we studied daily observations of mean, minimum and maximum
15 temperatures (T_{avg} : 29, T_{min} : 12 and T_{max} : 10 stations), snow depth (SD: 43 stations) and
16 streamflow (Q : 32 gauges), which were provided by *Hydrographischer Dienst Tirol (Innsbruck)*,
17 *AlpS GmbH (Innsbruck)*, *Zentralanstalt für Meteorologie und Geodynamik (Vienna)* and *Tiroler*
18 *Wasserkraft AG (Innsbruck)*. T_{min} and T_{max} data was taken from the *HOMSTART* dataset
19 (homogenised station datasets, Nemeč et al., 2012). Hourly temperature data was only available
20 for the *Vernagt* station, which was provided by the *Kommission für Glaziologie (Munich)*,
21 Escher-Vetter et al., 2014). The IDs of the T and SD stations were generated from the rank of
22 station altitude, Q station IDs from the rank of mean watershed altitude, i.e., the higher the
23 adjacent watershed, the lower the ID. Prior to the analysis, streamflow records were normalised
24 by catchment area (flow rate per unit area).

25 Eight of the 32 catchments analysed are nested. We used the approach that was applied as well in
26 Birsan et al. (2005): To guarantee spatial independence of the station data, we checked for a
27 considerable increase in watershed area among the corresponding gauges. Only the station pair
28 Innergschlöß (39 sq km) and Tauernhaus (60 sq km) did not meet the requirements as defined in
29 Birsan et al. (2005). However, as these basins were necessary to increase the number of

1 catchments with glacial influence and the requirements of station independence were not violated
2 too strongly, we left them in the dataset.

3 The characteristics of the watersheds and their IDs are summarized in Table 1. A map of the
4 study area together with the meteorological stations used in this study and annual streamflow
5 trends is provided in the results section (Fig. 1).

6 In Kormann et al. (2014), precipitation trends were studied as well. However, no clear and
7 coherent significant change patterns could be identified in this study (similar to e.g. Pellicciotti et
8 al. (2010) or Schimon et al. (2011)). Precipitation changes might exist, but cannot be detected
9 which is due to methodological limitations stemming from a low signal-to-noise ratio.

10 We selected the period 1980-2010 for the data analysis. This ensured consistent data length for
11 all hydro-climatic variables and best data availability. In this period, the Greater Alpine Region
12 experienced a strong increase in air temperature by about 1.3 °C, compared to about 0.7 °C
13 between 1900 and 1980 (Auer et al., 2007). Furthermore, the magnitudes of streamflow,
14 temperature, snow depth and snowfall trends is strongest for this period within the study region
15 (Kormann et al., 2014).

16 All hydroclimatic datasets were checked by Austrian government officials via extensive
17 examinations and plausibility checks. We additionally ensured that no data inhomogeneities
18 remained. We further excluded streamflow records of catchments influenced by major
19 hydro-electric power production. Unfortunately, it was impossible to exclude all watersheds with
20 influences from hydro power stations, as water resources in Western Austria are used
21 extensively: Only in Tirol, there are approximately 950 small-scale hydro power plants of
22 differing type with a capacity lower than 10 Megawatts¹. However, by far most of the small
23 hydro power plants in Austria are run-of-river power plants (A. Egger (Tyrolean spokesman of
24 the association on small hydro power plants in Austria), personal communication, July 29, 2014).
25 These power plants do not have any pondage and thus there is no delay of river runoff. The rest
26 of the small hydro power plants are mostly equipped with 1-day water storage volumes, which
27 means there is a maximum delay of an average daily discharge amount, so the impacts on the
28 seasonal discharge behaviour are very limited.

29

1 <http://www.kleinwasserkraft.at/en/hydropower-tyrol> [July 2014]

1 **3. Methods**

2 **3.1 Trend detection and significance**

3 **3.1.1 The Mann-Kendall test and the Sen's Slope Estimator for trend detection**

4 The rank-based Mann-Kendall (MK) test was used to calculate the trend significance. The MK
5 test has been widely used in hydrological and climatological analyses (e.g. Gagnon and Gough,
6 2002, Birsan et al., 2005). Its advantages are the robustness concerning outliers, its high
7 statistical power and the fact that it does not require a certain distribution of the data. A further
8 description of the test is found in Helsel and Hirsch (1992).

9 The MK test in its original version has two main drawbacks: It accounts neither for
10 autocorrelation in one station dataset, nor for cross-correlation between datasets of different
11 stations. Both of them could result in the overestimation of an existent trend. Different methods
12 of taking this into account have been published in recent years: Concerning serial correlation, the
13 prewhitening method after Wang and Swail (2001) was applied: Lag-1 autocorrelation of the
14 data is first calculated and then removed in the case that it is higher than a certain significance
15 level (5 % in the present case). To account for spatial correlation in the data, a resampling
16 approach was applied (Livezey and Chen, 1983, Burn and Elnur, 2002): After randomly
17 shuffling the original dataset 500 times, all the resampled datasets were tested on trends in the
18 same way as the original one. The percentage of stations that tested significant with a local
19 significance level α_{local} in the original and in each of the resampled datasets was determined.
20 Based on the distribution of significant trends in the resampled datasets, the value was
21 calculated, which was exceeded with an $\alpha_{\text{field}} = 10\%$ probability. This value was then compared
22 to the percentage of significant results calculated from the original data. In case it is higher in the
23 original dataset, the patterns found are called “field significant”.

24 After calculating the significance of a trend, it is necessary to estimate its magnitude, i.e. the
25 slope of the trend. This was done by the robust linear Sen's Slope Estimator, which is computed
26 from the median of the slope between all possible pairs of data points (Helsel and Hirsch, 1992).
27 The Mann-Kendall trend test and the Sen's Slope Estimator provide complementary information
28 which we combined in illustrating the annual and seasonal trends. However, for reasons of

1 graphical display and continuity we restrict further analyses of the seasonal changes to the Sen's
2 slopes.

3

4 **3.1.2 Minimum detectability**

5 To cope with the problem that trends may exist but do not get detected because of a low
6 signal-to-noise ratio, we calculated minimal detectable trends (Δ_{MD}) as proposed by Morin
7 (2011). In this study, annual mean values and coefficients of variance were computed for global
8 precipitation data. Monte-Carlo simulations were carried out to generate trended data with
9 similar statistical features as the original one but with varying trends. By testing the trend
10 significance with the Mann-Kendall test, it was possible to estimate the minimal trend that was
11 detected as significant in 50 % of the cases. This absolute trend was named the minimal
12 detectable trend for a given station at a predefined α -level.

13 To calculate the Δ_{MD} of a given time series, we used the relationship that is represented in Fig. 6
14 of Morin, 2011. This is justified, as the minimal detectable trend does not depend on the
15 magnitude of the data. The plot displays the change of the probability of significant trend
16 detection versus signal-to-noise ratio (S/N) and record length (R), averaged over all previously
17 simulated trend values. For a given time series with a given record length it is then necessary to
18 look up the S/N that fits the red contour in the figure, i.e., the S/N at which the probability
19 computed reaches the 0.5 threshold. This S/N is then transferred into Δ_{MD} using the following
20 equation:

$$\Delta_{MD} = \frac{S/N * \sigma(X)}{R} \quad (1)$$

21 where $\sigma(X)$ is the standard deviation of the series of averaged observations (e.g. average annual
22 streamflow).

23

1 **3.2 Detection of annual streamflow trends and timing changes**

2 **3.2.1 Trends of annual streamflow averages**

3 First, we derived trends of annual streamflow to understand, whether the overall yearly water
4 availability changes while there is no information about seasonal changes. For this purpose,
5 annual averages of streamflow were calculated and later tested on trend significance and
6 magnitude. Next to this, minimal detectable trends of the annually averaged streamflow datasets
7 were calculated to find out, whether trends might not get detected due to a high signal-to-noise
8 ratio. Both significant and insignificant annual trends were then plotted on a map of the study
9 area and against the mean watershed altitude. Lastly, general change patterns were identified.

10

11 **3.2.2 Streamflow timing changes**

12 To detect changes of the timing of seasonal streamflow, we used the approach of Renner and
13 Bernhofer (2011). Here, a first order Fourier form model is fitted to runoff data x with n
14 observations per year (Stine et al 2009, Renner and Bernhofer 2011):

$$Y = \frac{2}{n} \sum_{j=1}^{j=n} e^{2i\pi(j-0.5)/n} (x_j - \bar{x}) \quad (2)$$

15 From the complex valued Y , we estimate the phase $\phi_x = \tan^{-1}(\Re(Y)/\Im(Y))$ from the real and
16 imaginary parts of Y . The annual phase of a variable describes the timing of its maximum within
17 a given year. The amplitude $A_x = |Y|$ describes its range. By applying this harmonic filter to
18 each year of data, we obtained a annual series of phase and amplitude which is further tested for
19 trends.

20 The approach was considered suitable for our purposes as well, as all of the annual hydrographs
21 in our dataset follow a distinct seasonal cycle with strong streamflow maxima in summer and
22 minima in winter. Fourier form models are a more robust measure than other commonly used
23 indicators, like e.g. the centre of volume (Whitfield, 2013, Renner and Bernhofer, 2011). For
24 further reading on this method, see Stine et al. (2009).

25

1 **3.3 Trend attribution via subseasonal examinations of streamflow changes**

2 **3.3.1 Trends and characteristic dates**

3 To understand the relationship between streamflow trends and the variables that cause these
4 trends, we derived high temporal resolution trends of streamflow on the one hand as the target
5 variable and both (1) the trends and (2) characteristic dates (CDs) of explanatory variables on the
6 other hand. We assume that it is possible to represent certain processes via these trends and the
7 CDs. If streamflow trends and the trends and CDs of temperature and snow depth occur at the
8 same time, we suppose that this might be an indicator for one of the causes of the Q trends.

9 (1) Initially, trends in daily resolution were derived. This approach enables the detection of finer
10 temporal changes compared to the conventional annual or seasonal Mann-Kendall trend test. The
11 30-day moving average (30DMA) trends of Q , T_{mean} , T_{min} and T_{max} and SD were partly calculated
12 and partly taken from Kormann et al. (2014): At first, the station dataset under consideration was
13 filtered using a 30-day moving average. Then a time series of each DOY for the years
14 1980–2010 is derived which we then tested for trends. This procedure yields a 365-value dataset
15 per station, which provides information on significance and magnitude of the 30DMA trend for
16 every day of the year. These series allowed us to pinpoint the emergence, direction and
17 magnitude of trends within the course of the year. In addition, daily field significances inform
18 during which DOYs the trend patterns found were overall significant. The approach of trend
19 detection via moving averages was similarly applied in Western US by Kim and Jain (2010) and
20 Déry et al. (2009), however, they used only 3-day and 5-day moving averages and they only
21 analysed trends in streamflow. Contrary to that, the 30-day moving average windows reduce
22 daily fluctuations considerably. With this, the influence of single events on a specific day of
23 year, which might cause erroneous trends, is reduced as well. The 30DMA trends thus yield
24 more robust trends.

25 (2) Next to the trends, characteristic dates of the annual cycle of Q , T_{mean} , T_{min} and T_{max} and SD
26 were derived. To calculate these CDs, all datasets were first smoothed by a 30-day moving
27 average. Through this, comparability to the 30DMA trends is ensured and a more robust estimate
28 of the CD is obtained because of reduced fluctuations. Then we calculated the mean annual
29 cycles for each variable and each station for the years 1980 to 2010, in a daily resolution.

1 Afterwards we selected the characteristic dates: For streamflow, the DOY of the overall annual
2 maximum streamflow ($\overline{DOY_{Q_{max}}}$) was chosen. With regard to the CDs of T_{mean} , T_{min} and T_{max} ,
3 we selected the average DOY when temperature passes the freezing point in spring and autumn
4 ($T = 0\text{ }^{\circ}\text{C}$ (mean DOY when $T > -0.2$ and $T < +0.2\text{ }^{\circ}\text{C}$)), as this point is crucial for multiple
5 hydroclimatological processes in the watershed ($\overline{DOY_{0^{\circ}T_{mean|min|max}}}$). Concerning snow depth,
6 the average DOY of the annual maximum snow depth was chosen to indicate the date of the
7 average start of the snowmelt in the watersheds ($\overline{DOY_{SD_{max}}}$).
8 The CDs of T_{mean} , T_{min} and T_{max} and SD had to be fitted to the average altitudes of the watersheds.
9 For this purpose, the average CD of each station was depicted as a function of station altitude. As
10 all the CDs analysed had an approximate linear relationship with altitude, the DOYs of the trends
11 and thresholds were transferred to the mean altitudes of the watersheds on the basis of a linear
12 regression model.
13

14 **3.3.2 Linear model identification**

15 An empirical statistical model is another tool for analysing which processes cause streamflow
16 trends. Hence, a multiple linear model was fitted to the 30DMA streamflow trends found in the
17 study region. This was restricted to the period between the beginning of March and
18 mid-September (DOY 60 to DOY 250), where 85 % of the total annual streamflow and 84 % of
19 the seasonal streamflow trends (based on absolute trend magnitudes) occur. It is approximately
20 the time between the average annual snow depth maximum (top-of-winter) in spring, before
21 snow and glacier melt starts, and the average start of snow depth increases in autumn.
22 Based on the previous results of this study, we gathered all possible variables which then served
23 as predictor variables (independent variables): Next to catchment properties such as mean
24 watershed altitude, glacier (forest etc.) percentage or decrease of glaciated area, we used linear
25 regression to transfer long-term average temperatures to the mean watershed altitudes. This
26 means, the assignment of the average temperatures was based on regionally derived temperature
27 lapse rates. We decided to not use snow data as the assignment of snow depth to certain altitudes
28 is highly uncertain. The $\overline{\Delta T}$ time series were 30DMA temperature trends averaged over all
29 available stations. This was feasible, as similar trends concerning timing and magnitude occur at

1 all stations analysed. Similar to the earlier analyses, all the datasets of hydroclimatological
2 variables were filtered on the basis of 30-day moving averages beforehand.
3 Different combinations were first tested via a heuristic search based on the *R*-package *glmulti*
4 (version: 1.0.7, Calcagno and de Mazancourt, 2010). Later, the model with the best performance
5 in terms of an information criterion was chosen.

6

7 **3.3.3 Hourly trends**

8 To get an impression of the changes on a subdaily scale and support the previous statements
9 based on seasonal trends, we analysed hourly streamflow and temperature data. As there were
10 only a limited number of stations available, we selected several gauges that were representative
11 for the area (*Gepatschalm, Obergurgl, Tumpen*; ID no. 3, 4 and 9; Table 1) with differing glacier
12 percentages (39.3 %, 28.2 % and 11.8 %). Obergurgl and Tumpen are both located in the Ötztal
13 valley, Gepatschalm is located in an adjacent valley. The data was available only in the period
14 1985 to 2010 (compared to 1980 to 2010 for the earlier analyses). The applied methods are
15 analogous to the previous analyses: For each station, DOY and hour, 30DMA trends were
16 calculated and depicted in a similar way to the seasonal 30DMA trends. However, compared to
17 the earlier plots, the ordinate is now changed from rank of station altitude to hour of day.
18 Accordingly, the averages of one day's trend magnitudes (the entire y-axis) are the same values
19 as the trend magnitudes of one station in the earlier plot.

20

21 **4. Results**

22 The results and discussion sections are structured according to the analyses that were conducted
23 (for a schematic illustration, see appendix A.1). In the first part, we analysed trends of *annually*
24 *averaged streamflow and trends of the results of the Fourier form models*. For this purpose, three
25 different approaches were used: (1) mapping of annual trends in the study area, (2) analyses of a
26 potential altitude dependency of the annual trends and (3) analyses of trends of the phase and the
27 amplitude of the annual streamflow cycle. Based on the outcomes of this analyses, we defined
28 research hypotheses (see introduction section).

1 To support these hypotheses, we derived *trends of seasonally averaged streamflow* in the second
2 part, of not only streamflow but also (mean, maximum and minimum) temperature and snow
3 depth. These seasonal trends were then further applied in the attribution approaches: (1) a
4 combination of characteristic dates and trends, (2) a multiple regression model for streamflow
5 trends and (3) hourly trends.

6

7 **4.1 Detection of trends based on annual averages, phases and amplitudes**

8 Fig. 1 displays the annual streamflow trends (ΔQ_{year}), which were calculated from the change
9 per year divided by mean annual streamflow, on a map of the study area. Roughly two-thirds of
10 ΔQ_{year} in the study region are not significant at a significance level of $\alpha=0.1$, and no field
11 significance was detected. The mapped trends neither depict any clear spatial trend pattern, nor
12 show strong overall changes in Alpine hydrology. However, when presenting all annual
13 streamflow trends, significant and insignificant, versus station ID as a rank of mean watershed
14 altitude, another impression stands out (Fig. 2): It seems that higher-altitude watersheds depict
15 mostly positive trends, whereas lower-altitude watersheds show negative trends. The watersheds
16 at mid-altitudes show both positive and negative trends. Only nine out of 32 trends, where the
17 change signal is high enough compared to the noise, are significant. The other ones are below the
18 corresponding Δ_{MDS} . This applies both for trends calculated from the change per year divided by
19 mean annual streamflow (Fig. 2 a) as well as for trends derived from absolute values (Fig. 2 b).
20 Concerning the phase of streamflow, there is a clear signal of decreasing trends at higher stations
21 (Fig 2 c), representing an earlier onset of spring freshet. At lower stations, phase trends are
22 insignificant, mostly due to higher signal-to-noise ratios, which increase the minimal detectable
23 trend (dashed lines). The trends of the streamflow amplitudes show a similar behaviour to the
24 trends of annual Q averages, but shifted to mostly negative trends (Fig 2 d): In general,
25 amplitudes are decreasing, but less so at higher stations and more so at lower stations.
26 All the trends mentioned above show an explicit correlation with the mean watershed altitude,
27 which does not depend on trend significance (Table 2). Note that the Pearson's correlation
28 coefficients of significant trends are based on fewer values, so in this case higher correlation
29 coefficients are easier to obtain. All of the correlations tested significant at the $\alpha = 0.1$ level.

1

2 **4.2 Trend attribution via subseasonal trends**

3 **4.2.1 Trends and characteristic dates of streamflow**

4 As already found in Kormann et al. (2014), coherent 30DMA streamflow trend patterns appear
5 when plotted against the time of year and altitude (Fig. 3a). We refer to the groups discernible in
6 these plots as “trend patterns”. Streamflow clearly rises in spring, followed by decreases in
7 summer; both trend patterns depend on watershed altitude. Another obvious pattern is the
8 positive one in autumn, roughly from October to December; this one was not found to be
9 altitude-dependent. Over most of the time, the 30DMA trends are field-significant (Fig. 3a), *bar*
10 *above diagram*), meaning the trend patterns as a whole are statistically more frequent than
11 expected by random chance.

12 At higher-altitude basins, significant Q trends in annual averages (ΔQ_{year}) were found
13 especially where ΔQ_{30DMA} in spring have high values (Fig. 3a), *bar on the right*). At lower
14 stations, only two significant ΔQ_{year} were detected, both at watersheds where hardly any
15 positive ΔQ_{30DMA} were detected.

16 When analysing all 30DMA streamflow trends (Fig. 3b), not only the significant ones, the
17 designated trend patterns are even more obvious. An additional positive trend pattern occurs in
18 mid-August at higher stations, though this one is less evident than the others.

19 The CD, that indicates the DOY when the long-term annual streamflow peak occurs ($\overline{DOY}_{Q_{max}}$
20), is often found after the increasing trends in spring and before the decreasing trends in summer
21 (Fig. 3b), which is especially true for lower stations. This means that increasing Q trends mostly
22 occur during the rising limb, and decreasing ones during the falling limb of the seasonal
23 hydrograph. These patterns correspond to a shift in the hydrograph and thus a decreasing trend in
24 the phase of streamflow timing.

25

1 **4.2.2 Trends and characteristic dates of temperature and snow depth**

2 The analysis on elevation dependence of the CDs of T and SD derived from climate stations is
3 presented in Fig. 4. The average DOYs of daily T_{mean} , T_{min} and T_{max} surpassing the freezing point
4 ($\overline{DOY}_{0^\circ T_{\text{mean}/\text{min}/\text{max}}}$) all depend on altitude, in spring as well as in autumn (Fig. 4a and b). The
5 same applies for the average DOY of the annual snow depth maximum ($\overline{DOY}_{SD_{\text{max}}}$, Fig. 4c).
6 Almost all the characteristic dates show a linear relationship with station altitude. Thus this
7 linear relation is being used to establish a representative, long-term CD for each watershed using
8 the mean catchment altitude.

9 Regarding trends, there are differences between the T_{min} , T_{max} and T_{mean} trends, but these
10 differences mostly concern the trend magnitude, not its direction or timing (Fig. 5 a, b and c).
11 Comparing single stations with each other, it is obvious that the T trends appear in temporal
12 clusters that start and end during similar DOYs. Four main patterns of field-significant positive T
13 trends are evident: 1) mid-March until the beginning of May, 2) mid-May until the end of June,
14 3) the beginning of July until mid-August, and 4) the beginning of October until mid-November.
15 The T_{max} trends are roughly twice as intense as the ones for T_{min} and T_{mean} , but field significance
16 was detected only in two of the four highlighted segments (upper bar in Fig 5). For most of the
17 stations, the magnitude and days of occurrence are similar, meaning there is no altitude
18 dependence of the T trend signal.

19 Fig. 5d shows the analogous trend results for the explanatory variable snow depth (SD). Strong
20 negative SD trends dominate the results; however, some positive trends occur at two upper
21 stations and around November at many of the stations. One main cluster of field-significant
22 trends in spring can be distinguished, which also indicates that local significant trends were
23 found only in spring.

24

25 **4.2.3 Comparison of the timing of trends and characteristic dates of streamflow** 26 **with those of temperature and snow depth**

27 *Spring* ($\overline{DOY}_{0^\circ T_{\text{maxSpring}}}$ to $\overline{DOY}_{0^\circ T_{\text{minSpring}}}$): $\overline{DOY}_{0^\circ T_{\text{maxSpring}}}$ and $\overline{DOY}_{SD_{\text{max}}}$ appear during
28 similar days as the first Q trends (Fig. 5e). Between $\overline{DOY}_{0^\circ T_{\text{maxSpring}}}$ and $\overline{DOY}_{0^\circ T_{\text{meanSpring}}}$, the
29 Q trend magnitudes further increase, most of them in shifts, i.e. first the lower basins around

1 early March and the later ones in April. In April, there is a general major peak in the observed
2 streamflow trends at basically all of the watersheds. This is also the time when field-significant
3 SD trends turn up at the majority of stations (Fig. 5d). During this period, it seems that there is an
4 elevation-dependent trend pattern between $\overline{DOY_{0^\circ T_{max}Spring}}$ to $\overline{DOY_{0^\circ T_{min}Spring}}$ superposed by
5 an elevation-independent one.

6 The overall strongest Q trends occur at high-lying watersheds after the average daily T_{mean} is
7 positive and when T_{min} is still negative. T trends are also at their highest levels during this time of
8 year, and the dynamics of the T trends resemble the ones in the Q trends with overall maxima
9 between end of May and beginning of June. Pearson's r between all single streamflow trends
10 from $\overline{DOY_{0^\circ T_{mean}Spring}}$ to $\overline{DOY_{0^\circ T_{min}Spring}}$ and the corresponding glacier percentage in the
11 watershed was calculated at 0.74, which means the strongest Q trends turn up mostly at
12 watersheds that are highly glaciated.

13 Some trends at mid-altitude watersheds stand out with high magnitudes and long persistence (at
14 gauges No. 8, 12, 17). All these rivers are fed by glaciers that originate from the *Hohe Tauern*
15 region (eastern side of the study region, cf. Fig. 1).

16

17 *Summer* ($\overline{DOY_{0^\circ T_{min}Spring}}$ to $\overline{DOY_{0^\circ T_{min}Autumn}}$): During summer, many of the Q trends observed
18 are negative, with the strongest ones at lower basins after T_{min} has crossed the freezing point in
19 spring. At higher, glaciated watersheds, negative Q trends occur only after positive Q trends have
20 diminished. Field significant T trends go along with these Q trends; both of them are especially
21 strong from mid-May until mid-June.

22

23 *Autumn* ($\overline{DOY_{0^\circ T_{min}Autumn}}$ to $\overline{DOY_{0^\circ T_{max}Autumn}}$): In autumn there are two main patterns with
24 opposing signs: Negative Q trends at higher-altitude watersheds in September and slightly
25 positive Q trends at all watersheds around October. In September, the negative Q trends coincide
26 with negative T trends. In October, positive field-significant trends in T_{mean} and T_{min} were
27 detected. $\overline{DOY_{0^\circ T_{max}Autumn}}$ and $\overline{DOY_{0^\circ T_{min}Autumn}}$ do not border the Q trends as clearly as in spring.

28

1 *Winter* ($\overline{DOY_{0^{\circ}T_{maxAutumn}}}$ to $\overline{DOY_{0^{\circ}T_{maxSpring}}}$): All throughout winter, there is hardly any
 2 streamflow persisting in the highest watersheds. This is also reflected in the fact that there are
 3 only few trends at the upper 20 watersheds. Contrary to that, minor streamflow trends exist at
 4 lower watersheds; however, there is no clear positive or negative pattern and trend magnitudes
 5 are small.
 6

7 **4.2.4 Empirical statistical model for streamflow trends**

8 The heuristic model selection based on the information criteria identified the most relevant
 9 explanatory variables. The best performance (the adjusted R^2 was calculated as 0.70) was
 10 achieved with the model in Eq. 3. Note that we normalized the trend of streamflow at a specific
 11 DOY (ΔQ_{30DMA}), as well as the first derivative of the seasonal 30DMA Q average ($\overline{Q_{30DMA}}$)
 12 by the long-term average streamflow at a specific DOY ($\overline{Q_{30DMA}}$).

13

$$\frac{\Delta Q_{30DMA}}{\overline{Q_{30DMA}}} = 0.0017 - 0.096 \overline{\Delta T_{min}} + 0.0036 \frac{\overline{Q_{30DMA}}}{\overline{Q_{30DMA}}} + 0.59 \frac{A_{ice}}{A_{tot}} \overline{\Delta T_{min}} \quad (3)$$

14

15 From the a-priori selected explanatory variables, we found that only 3 variables are required to
 16 predict the streamflow trend at a specific day of the year: minimum temperature, the first
 17 derivative of streamflow indicating rising or falling streamflow conditions as well as the
 18 percentage of glaciated area in a watershed (A_{ice}/A_{tot}) multiplied by the 30DMA T_{min} trend in $^{\circ}C$
 19 per year for the corresponding DOY, averaged over all available stations.

20 The prerequisites of a linear model (homoscedascity, normally distributed residuals) were
 21 checked via standard diagnostic plots. The large majority of the predicted trend values were in
 22 accordance with the observed ones (Fig. 6); only several very high values ($> 4\%$) could not be
 23 simulated well. All of these values were found at the gauge with the highest percentage of
 24 glaciated area in the watershed (ID 1, Vernagt). Also at this gauge, there are several occasions
 25 when observed trends are zero although the model predicts that there is a trend. This happens
 26 during earlier DOYs, when there is no discharge as all water in the basin is still frozen.

1

2 **4.2.5 Analysis of hourly streamflow trends**

3 The overall results of the hourly T and Q trend analysis show similar structures to the seasonal
4 one (Fig. 7). Concerning Q , there are certain periods when subdaily dynamics in Q trends are
5 obvious, like the period from mid-May until mid-June. During other periods, there is hardly any
6 difference between the trends at different times of day.

7 More specifically, from mid-March to early May, there is merely a diurnal dynamic in the Q
8 trends. Positive T trends without any explicit diurnal dynamic occur at the same time.

9 Contrasting with this, from mid-May until mid-June there is a clear dependency between the
10 positive trends in the afternoon, the time of day and the watershed analysed: The lower the
11 watershed and the smaller the glacier percentage, the later the Q trends occur and the lower are
12 their magnitudes.

13

14 **5. Discussion**

15 **5.1 Detection of trends based on annual averages, phases and amplitudes**

16 The positive (and often significant) annual streamflow trends at higher-altitude, glaciated
17 watersheds might be a sign that glaciers in Western Austria are still in the phase, where overall
18 streamflow still rises due to increasing glacial melt. This corresponds well with other studies in
19 the European Alps (Pellicciotti et al., 2010, Bard et al., 2011, Braun and Escher-Vetter, 1996).

20 Contrary to that, the annual Q trends at lower-altitude basins are mostly insignificant, but
21 negative. Rising temperatures change hydroclimatic conditions in the basins, resulting in e.g.
22 shorter winters, higher evapotranspiration, higher infiltration and alternating storage capacities
23 (Berghuijs et al., 2014). Hence, less water contributes directly to runoff, which might be a
24 potential cause for the negative annual trends observed in lower-altitude basins.

25 The ambiguous change signals of annual Q trends at mid-altitude watersheds with little or no
26 glacier cover might be a result of a balancing effect of increased glacial melt and rising
27 evapotranspiration. Hence, trends are mostly lower than the corresponding minimal detectable

1 trends, so in many cases, no significance is detected. This goes along with Birsan et al. (2005),
2 who found decreasing trends in basins with a glacier cover of less than 10 %.

3 The present analysis of annual streamflow trends shows once more that it is important to also
4 include insignificant trends in the interpretation of the results. It might not have been possible to
5 find the overall altitude-dependent patterns when only looking at significant results. However, it
6 is crucial to interpret the insignificant trend results more carefully.

7 The analyses of Q phase and Q amplitude highlight the different behaviour of higher- and
8 lower-altitude watersheds under climate change. We observe a significant shifts towards earlier
9 streamflow timing in the upper catchments, whereas the amplitudes decrease in the lower
10 catchments. However, the Fourier form models are increasingly uncertain in lower catchments
11 where the annual hydrograph deviates from a harmonic function. Therefore, a seasonal trend
12 analysis is required to detect potential regime changes.

13

14 **5.2 Trend attribution via subseasonal trends**

15 **5.2.1 Comparison of the timing of trends and characteristic dates of streamflow** 16 **with those of temperature and snow depth**

17

18 *Spring:* The ambiguous structure of the mid-January to April streamflow increases (altitude
19 dependent vs. altitude independent trends) is possibly caused by the following two mechanisms:
20 On the one hand, temperatures need to rise above the freezing level to allow for snowmelt
21 initiation. This DOY depends on the altitude of the snowpack (e.g. Reece and Aguado (1992)
22 found an altitudinal melt onset gradient of 4 days per 100 m in the Sierra Nevada). With T trends
23 occurring during the whole spring, snowmelt initiation shifted to earlier DOYs, which probably
24 caused the elevation-dependent trend pattern.

25 On the other hand, the average spring rise of streamflow occurs at most of the watersheds in the
26 study region during similar days of the year (see Kormann et al., 2014), which implies that
27 snowmelt starts simultaneously at different altitudes. Hence, it seems that snowmelt in our study
28 region is highly driven via weather patterns and their hydrological effects such as rain-on-snow
29 events that influence e.g. whole valleys and not just single altitude bands. Garvelmann et al.

1 (2014) showed that snowmelt is strongly driven via rain-on-snow events and highly depends on
2 the previous moisture of the snow pack. Lundquist et al. (2004) observed altitude-independent
3 snow melt in single years. With increasing T , rain-on-snow events might have turned up earlier
4 in the season, thus causing the elevation-independent trend pattern during spring.
5 It is possible, that in some years, the first mechanism is stronger, and in other years the second
6 one, with both of them moving to earlier DOYs.
7 The May to June streamflow increases at upper watersheds are by far the strongest Q trends that
8 were found. The similar dynamics of T and positive Q trends during this period suggest a
9 strongly temperature-driven trend cause. Furthermore, not only the high correlation of the Q
10 trend magnitude with watershed glacier percentage but also the fact, that many trends in
11 glaciated basins still persist when average T_{\min} has already been above 0°C for many days (see
12 next section), indicate that these pattern might be caused by increasing glacial melt. The strong Q
13 trends of watersheds in the Hohe Tauern region suggest a particularly high glacial meltdown in
14 this area.
15 All these evidences suggest that the first spring trend pattern is caused by both earlier snowmelt
16 and less snowfall (Kormann et al., 2014) and the second one is a result of shrinking glaciers due
17 to rising temperatures. Anyway, one has to keep in mind that it is practically impossible to
18 explicitly separate trends caused by snow melt and the ones caused by glacier melt, as melt at
19 lower glacier parts already starts while the upper parts are still covered with snow.
20 At a first glance, glacier melt in May might appear as very early in the year when looking at
21 seasonal streamflow composition. However, one has to note that the *trends* in glacier melt should
22 not be confused with the *actual amount* of glacier melt: The main icemelt is happening later in
23 the year, however, the strongest trends turn up earlier. These Q trends are highly connected to
24 temperature trends, which are as well strongest during this time of year (cf. Fig. 5). The results of
25 modelling approaches (e.g. Alaoui et al., 2014) confirm our interpretations and suggest that
26 glacier melt starts even earlier in the year.
27
28 *Summer:* In summer, the snow reservoir has already emptied out in most of the watersheds. The
29 negative Q trends during this time of year are possibly part of the effects of earlier snowmelt
30 timing on streamflow. This shift causes first rising and directly afterwards dropping streamflow

1 trends in spring and summer, which were similarly found for watersheds in western North
2 America by other daily resolved trend analyses (Kim and Jain, 2010, Déry et al., 2009).
3 However, to fully attribute summertime Q decreases, it would be necessary to separate the
4 effects of shifts in snowmelt timing from the effects of lower snow accumulation (and with this,
5 lower snowmelt volumes). This task had been addressed in Déry et al. (2009) by a simple model
6 approach. However, a separation of these effects based on analyses of other observed variables is
7 difficult, as negative Q trends in summer might also have other causes such as higher infiltration,
8 rising evapotranspiration and changing storage conditions (Berghuijs et al., 2014).

9 At higher-altitude basins, the negative summertime Q trends are balanced to a certain degree by
10 positive trends due to excess water from glacial melt, which is evident via trends that persist far
11 longer than the $\overline{DOY_{0^\circ T_{minSpring}}}$. This superimposition might also cause positive Q trends in
12 mid-August at upper stations, maybe because the negative summertime trends have already
13 weakened then. According to Stahl and Moore (2006), the biggest difference in streamflow
14 trends of glaciated and unglaciated basins is found during the month of August. However,
15 contrasting to their study, we found mainly increasing August Q trends at glaciated watersheds
16 and slightly decreasing ones at unglaciated watersheds.

17 The altitude dependency of the timing of $\overline{DOY_{Q_{max}}}$ highlights the need for highly resolved,
18 subseasonal trend analyses: As upward trends generally occur before and downward trends occur
19 after $\overline{DOY_{Q_{max}}}$, a separation of trend statistics in periods of 3-month (spring, summer, autumn,
20 winter), as it is usually done in trend studies, might produce ambiguous trend results especially
21 in summertime.

22

23 *Autumn:* Cahynová and Huth (2009) showed that significant increases in cyclonic circulation
24 types are the major cause for autumn temperature decreases. These negative T trends in turn
25 might have caused the Q decreases at higher-altitude basins in September, as during this time of
26 year, the glacier is exceptionally not melting but accumulating. These effects are possibly
27 increased by the negative summertime Q trends due to snow decreases in the previous winter and
28 earlier melt. Contrary to that, during October, rising T_{mean} and T_{min} might cause less snowfall and
29 less snow to be accumulated and hence generate more rainfall-driven runoff during this time of

1 year. This generally goes along with the interpretations in earlier literature (e.g. Déry et al.,
2 2005).

3

4 *Winter:* During winter, T_{\max} is far below zero, so on average no melt processes are possible.
5 However, temperatures might reach above zero in the lower catchment areas of certain
6 watersheds, so positive Q trends could be caused through lower snow accumulation in these
7 watersheds. The negative trends in absolute snow depth might have been caused at the beginning
8 of the winter, so it is plausible that these have no effect on streamflow during mid-winter. These
9 interpretations generally go along with e.g. Scherrer et al. (2004), who attributed SD decreases at
10 lower-altitude stations to T increases rather than changes in precipitation patterns.

11

12 **5.2.2 Empirical statistical model for the identification of streamflow trends**

13 The multiple linear model is able to simulate daily streamflow trends sufficiently well. The
14 predictor $\overline{Q_{30DMA}}$ accounts for both positive Q trends in the rising limb of the annual Q cycle
15 (before the annual maximum) and for negative trends that turn up in the falling limb (cf. Fig. 3).
16 Reinterpreted as a trend, the term $\overline{Q_{30DMA}}$ corresponds to a shift in earlier streamflow timing of
17 one day per year. The coefficient (0.36) in our model adjusts this term to the shift found in our
18 data. For the 30-year study period, this counts up to a shift of 10.8 days of earlier streamflow
19 timing, which is similar to shifts reported in the literature. For example, Renner and Bernhofer
20 (2011) report an shift of 10 to 22 days earlier timing (comparing 1950–1988, and 1989–2009) in
21 the runoff ratio for catchments in the low mountain ranges of Saxony, Germany. Déry et al.
22 (2005) found that annual peak snowmelt discharge appears roughly 8 days earlier (study period
23 1964–2000), Stewart et al. (2005) detected a shift of 6–19 days (1948–2003), both in North
24 America and based on timing measures such as 'centre of volume'. However, depending on
25 factors like the study period, region and the methods used, results in previous literature differ
26 strongly.

27 The predictor ' A_{ice}/A_{tot} ' considers the increased excess water from glacial melt in the model. The
28 selection of this term and not that of e.g. 'decrease of glaciated area' (which has been tested as
29 well) supports the findings of Weber et al. (2009): As glacial melt mostly occurs at the surface,

1 the quantity of melt water generally behaves proportionately to the extent of glaciated area in the
2 watershed, independent of the underlying glacier thickness.

3 The glacial melt is driven via the temperature increases, hence the glacier term includes the
4 30DMA temperature trends. As the ' $A_{ice}/A_{tot} \overline{\Delta T_{min}}$ ' term enters the model with a positive
5 coefficient, one can assume that the majority of the glaciers have not yet reached the point when
6 overall streamflow decreases due to diminishing glacier mass.

7 The additional single term ' $\overline{\Delta T_{min}}$ ' has a negative coefficient, and hence might account for the
8 negative trends in summertime caused by increased ET, higher infiltration and decreased snow
9 cover accumulation. The selection of $\overline{\Delta T_{min}}$ instead of $\overline{\Delta T_{max}}$ is somehow surprising, as one
10 might expect many of the streamflow trends to be strongest during daytime, when temperatures
11 are at their highest. Indeed, the selection makes sense: The ground is potentially frozen once T_{min}
12 falls below zero. If this is the case, additional energy is necessary for melting during daytime.
13 With a rise in T_{min} , energy that is not needed any more for melting is now available for
14 atmospheric warming in addition to $\overline{\Delta T_{min}}$ alone.

15 The advantage that only little input data is necessary has also some drawbacks: As the model is
16 very slim, it only captures the main factors that could cause streamflow trends in highly alpine
17 catchments. Contributors such as changes in groundwater or precipitation are not accounted for
18 explicitly, only via their response to the other predictors. In autumn, the model is not able to
19 simulate the actual trends adequately either. However, these trends are small in magnitude and
20 do not influence the overall statements too much.

21 Furthermore, we found significant autocorrelation in the residuals, as the Durbin-Watson statistic
22 indeed indicated. This is violating the assumptions of independence of linear regression, which
23 often happens when fitting models to time series with a seasonal cycle. The autocorrelation in the
24 residuals precludes statements on confidence bands and significance tests: The standard errors of
25 the regression coefficients are potentially too small, which pretends higher model precision.
26 However, our model stands as an approximation only. We are aware that the model is not
27 perfect, as it is impossible to find all specific causes that explain the streamflow trends in our
28 study region. The model is able to simulate streamflow trends sufficiently well, providing further
29 hints on the causes of Q trends.

1

2 **5.2.3 Analysis of subdaily streamflow trends**

3 The hourly Q trend analysis supports the findings of the earlier analyses. Going into detail, the
4 patterns found might occur for the following reasons: Due to the relatively low albedo of glacial
5 ice (~0.3 to 0.5) compared to snow (~0.7 to 0.9, Paterson, 1994), glacial melt depends stronger
6 on incoming radiation than snowmelt. Climate change results in earlier snow-free conditions on
7 glaciers, which in turn cause earlier glacial melt during noontime. The resulting Q trends are
8 temporally delayed with increasing distance from the glacier and their magnitudes decrease with
9 decreasing watershed altitude. This might be due to a generally lower percentage of glaciated
10 area in the lower-altitude basins and a balancing effect of the negative Q trends which is caused
11 by earlier snowmelt, lower snow accumulation and rising ET.

12 In this context, it is noteworthy that there is no clear subdaily dynamic in the negative trends
13 during DOYs with T increases: With rising ET, one would expect stronger negative Q reductions
14 at noon due to the maximum necessary radiation input. This is either balanced via glacial melt or
15 the magnitude of the changes is too small compared to the reductions due to the shift of
16 snowmelt to earlier DOYs.

17

18 **5.2.4 Synthesis of the streamflow trend attribution approach**

19 In the following we synthesize the streamflow trends and potential causes. The overall findings
20 are illustrated with three representative catchments. Fig. 8(a) represents a typical higher-altitude
21 watershed (Gepatschalm, 2880 m, 39.3 % glaciated), (b) a mid-altitude, little glaciated watershed
22 (See i. P., 2303 m, 1.6 % glaciated) and (c) a lower-altitude, unglaciated watershed (Ehrwald,
23 1467 m), which are depicted along with the detected trends and their probable main drivers. Our
24 seasonal analyses support the hypotheses that we proposed in the introduction section: The
25 subseasonal structure of streamflow trends in higher-altitude, glaciated watersheds corresponds
26 well with the one that might stem from glacier wastage. The overall annual 30DMA trend
27 integral over time (and thus the annual trend) is positive, as additional water in spring enters the
28 basin (Fig. 8 a). In lower-altitude watersheds, especially summertime decreases lead to an overall
29 negative annual trend integral (Fig. 8 c). In case the annual 30DMA trend integral over time is

1 close to zero, the trends are caused by shifts rather than by changes of the overall streamflow
2 amount (Déry et al., 2009). This might be the case in mid-altitude, little glaciated watersheds,
3 where only small changes affect the annual hydrograph (Fig. 8 b).

4 In summary, the two main influences on alpine streamflow are the increased glacial melt and the
5 shift to earlier snowmelt, both driven via temperature increases. This is supported by many
6 studies in alpine regions, where drivers of streamflow changes were identified via modelling
7 approaches (e.g. Braun et al., 2010). Anyway, we want to emphasise that our analysis is based on
8 observed station data only. For this reason, we consider our statements concerning both the
9 detection and the attribution of the changes to be more robust than results obtained by
10 stand-alone model approaches. However, a few patterns still exist, where streamflow trend
11 attribution via temperature, glacier and snow depth changes is not sufficient and thus the need for
12 further research remains: For example, we could not explicitly identify the drivers of summer
13 streamflow decreases, especially with regard to ET increases. Also a model approach was not
14 successful to identify the role of rising ET on alpine hydrology for the past: Al Alaoui et al.
15 (2014) could not establish a link between changing hydrology and increased ET in the Swiss
16 Alps for the years 1983–2005. This was mainly due to the fact, that hydrological changes due to
17 rising ET were masked by changes caused by snow and glacier melt, which is similar in our
18 results.

19 Nevertheless, the shift of snowmelt to earlier DOYs and a higher rain/snow ratio has been
20 detected, also by other studies. With this, the watershed potentially receives more precipitation in
21 the form of rain which in turn possibly leads to higher annual infiltration and interception rates.
22 This water might be additionally available for evapotranspiration and vegetation growth and thus
23 will reduce seasonal - and with this annual - streamflow amounts. The study of Berghuijs et al.
24 (2014) supports this assumption for the contiguous US: They found observational evidence, that
25 a reduction in the percentage of snow in total precipitation goes along with decreases in average
26 streamflow.

27 Also higher transpiration rates through vegetation changes might be (additional) drivers of the
28 summertime streamflow decreases (Jones, 2011): In the study area, alpine livestock farming is
29 the main type of cultivation. The decline of this type of farming during the 1960s and 1970s

1 (Neudorfer et al., 2012) resulted in a still ongoing overgrowth of former grasslands, enhanced by
2 climate-change related land-use changes like increases of the timber line (Walther, 2003).
3 The empirical-statistical model established in the present study was proven to simulate
4 streamflow trends sufficiently well. Not only could it serve as a tool to gain deeper insight into
5 the processes that cause streamflow trends, but it could also be used to derive streamflow trends
6 in such alpine catchments, where only recently a gauge has been installed. Trends were found
7 to be quite uniform over the entire study region, so a climate station that is very close to the
8 watershed is not absolutely mandatory. The percentage of glaciated areas in the watershed can be
9 derived via glacier cadastres or satellite imagery.

10 The analysis of hourly streamflow trends supports the findings of the earlier analysis and shows,
11 that hourly resolved trend analyses can provide additional information on the changes in alpine
12 streamflow. Most of the gauging stations with hourly measurements have only been installed
13 since the eighties, so there has been hardly any research on the subdaily changes of streamflow
14 and there might be potential for further research.

15

16 **6. Summary and Conclusion**

17 The present study analyses trends and its drivers of observed streamflow time series in alpine
18 catchments, taking data from Western Austria as example. At first, trends of annual averages
19 were analysed: It was found that streamflow at higher-altitude watersheds is generally
20 increasing, while it is decreasing overall in lower-altitude watersheds. The following hypotheses
21 are proposed: (1) positive trends at higher, glaciated watersheds are caused by increased glacial
22 melt, (2) negative trends at lower, non-glaciated watersheds are caused by the hydrological
23 effects of rising temperatures such as less snowfall causing higher infiltration and in particular
24 increasing ET, and (3) many of the trends at watersheds in mid-altitudes are not identified,
25 because positive and negative trends cancel each other out and the final annual trend is too small
26 to be detected. To support these hypotheses, we attempted to attribute the trends, i.e. we tried to
27 identify the processes that cause the trends.

28 The biggest challenge in streamflow trend attribution is that streamflow measured at one gauge
29 integrates multiple processes all over the catchment area. This makes the identification of

1 individual drivers difficult as the final streamflow signal is a result of multiple processes where
2 upward and downward trends could balance each other out. The problem applies for many trend
3 analyses in the literature, where trends are calculated from averages over a certain period of time.
4 Therefore, daily resolution streamflow trends are derived, as they allow for a more precise
5 temporal localisation of the trends. The DOYs of these trends are then compared to average
6 DOYs of other hydroclimatological characteristics, such as the temperature surpassing the
7 average freezing point in spring, or e.g. DOYs of trends in snow depth. The DOYs of these
8 long-term characteristics fit well with the ones of the trends found in streamflow time series and
9 thus can be related to them. Additionally, an empirical statistical model and analyses of the
10 subdaily changes gave further hints for the causes of the streamflow changes in the study region.
11 With the present study, we have shown that the hydrological dynamics in alpine areas are
12 changing significantly. Still, looking at the yearly averages of streamflow data, the ongoing
13 change is masked by the fact that additional runoff caused by enhanced glacier melt and possibly
14 increased precipitation is counter-balanced by modifications of the water cycle such as higher
15 ET, less snowfall and rising infiltration in the vegetation season. These opposing forces may
16 balance out within catchments comprising higher and lower altitudes, because the increased
17 streamflow mainly prevails in higher areas while decreasing streamflow is mostly found in lower
18 areas. We are confident that we have identified a rather robust trend of hydrological change in
19 specific hydro-climatological regions, e.g. alpine catchments. Even though the changes are only
20 partially identifiable when analysing yearly averages, they can clearly be seen when studying
21 smaller time increments. This detailed analysis of high-resolution hydrological time series
22 follows Merz et al. (2012b), who called for a more rigorous data analysis in order to analyse
23 possible hydrological changes. The identified altered hydrological dynamics in the case of the
24 alpine catchments is driven mostly by temperature increases. This supports Bronstert et al., 2007,
25 who concluded that temperature increases, rather than precipitation changes, cause hydrological
26 changes which may be quite robustly detectable. A trend attribution of this kind is an important
27 step towards a scientifically sound assessment of climate change impacts on hydrology. A
28 proceeding step should be the process-based modeling of such hydrological systems (Bronstert et
29 al., 2009), which – in case the detected trends can be replicated by the model results – can further
30 sustain the findings concerning climate effects on alpine hydrological systems.

1 Our attribution approaches could possibly be applied to regions other than mountainous areas.
2 However, one must be aware that results might be rather different and/or less well identifiable if
3 changes are not as strongly temperature-driven as those in mountain regions. However, as stated
4 above, hydrological trend studies should attempt to not only detect but also attribute the trends.
5 For this reason, it is worth looking for attribution methods adapted to the particular local
6 condition. In any case, daily resolved trends are helpful to detect and attribute hydrological
7 regime changes in alpine catchments, which could be overseen by annual or trimonthly trend
8 assessment.

9

10 **Acknowledgements**

11 The authors express their gratitude to *Hydrographischer Dienst Tirol (Innsbruck)*, *AlpS GmbH*
12 *(Innsbruck)*, *Zentralanstalt für Meteorologie und Geodynamik (Vienna)*, *Kommission für*
13 *Glaziologie (Munich)* and *Tiroler Wasserkraft AG (Innsbruck)* for supplying local station data,
14 and to Efrat Morin (Hebrew University Jerusalem, Israel) and Gerd Bürger (University of
15 Potsdam, Germany) for inspiring discussions. We further thank Marius-Victor Birsan, Juraj
16 Parajka and two anonymous reviewers for their work as referees and to Peter Molnar as associate
17 editor. This study was kindly supported by the Potsdam Research Cluster for Georisk Analysis,
18 Environmental Change and Sustainability (PROGRESS) and the Young Scientists Exchange
19 Program (YSEP) in the framework of German-Israeli Cooperation in Water Technology
20 Research, both founded by the German Federal Ministry of Education and Research (BMBF).
21 The YSEP program was additionally founded by the Ministry of Science, Technology and Space
22 Israel (MOST).

23

24 **References**

25 Alaoui, A., Willmann, E., Jasper, K., Felder, G. Herger, F., Magnusson, J., and Weingartner, R.
26 (2014) Modelling the effects of land use and climate changes on hydrology in the Ursern Valley,
27 Switzerland . *Hydrol. Process.* 28, 3602-3614, doi: 10.1002/hyp.9895.

- 1 Auer, I., Böhm, R., Jurkovic, A., Lipa, W., Orlik, A., Potzmann, R., Schöner, W., Ungersböck,
2 M., Matulla, C., Briffa, K., Jones, P. D., Efthymiadis, D., Brunetti, M., Nanni, T., Maugeri, M.,
3 Mercalli, L., Mestre, O., Moisselin, J. M., Begert, M., Müller-Westermeier, G., Kveton, V.,
4 Bochnicek, O., Stastny, P., Lapin, M., Szalai, S., Szentimrey, T., Cegnar, T., Dolinar, M., Gajic-
5 Capka, M., Zaninovic, K., Majstorovic, Z., and Nieplova, E. (2007) HISTALP – Historical
6 Instrumental Climatological Surface Time Series of the Greater Alpine Region. *Int. J. Climatol.*,
7 27, 17-46.
- 8 Bard, A., Renard, B., and Lang, M. (2011) The AdaptAlp Dataset. Description, guidance and
9 analyses, Final Report, UR HHLY, Hydrology-Hydraulics, Lyon, 15 pp.
- 10 Barnett, T.P., Adam, J.C. and Lettenmaier, D.P. (2005) Potential impacts of a warming climate
11 on water availability in snow-dominated regions. *Nature*, 438, 303-309.
- 12 Berghuijs, W. R., Woods, R. A. and Hrachowitz, M. (2014) A precipitation shift from snow
13 towards rain leads to a decrease in streamflow, *Nat. Clim. Change* 775(4), 583-586,
14 doi:10.1038/nclimate2246.
- 15 Birsan, M.V., Molnar, P., Pfaundler, M., and Burlando, P. (2005) Streamflow trends in
16 Switzerland. *J. Hydrol.*, 314 (1-4), 312-329, doi: 10.1016/j.jhydrol.2005.06.008.
- 17 Blöschl, G., Viglione, A., Merz, R., Parajka, J., Salinas, J. L., Schöner, W. (2011) Auswirkungen
18 des Klimawandels auf Hochwasser und Niederwasser. *Österreichische Wasser- und*
19 *Abfallwirtschaft*, 63, 21-30.
- 20 Burn, D. H., and Elnur, H. (2002) Detection of hydrologic trends and variability. *J. Hydrol.*, 255,
21 107-122.
- 22 Braun, L. N., and Escher-Vetter, H. (1996) Glacial discharge as affected by climate change, in
23 *Interpraevent Internationales Symposium*, vol. 1, pp 65–74, Garmisch-Partenkirchen, Germany.
- 24 Braun, L., Weber, M., and Schulz, M. (2000) Consequences of climate change for runoff from
25 Alpine regions. *Ann. Glaciol.* 31(1): 19–25.
- 26 Braun, L., Escher-Vetter, H., Siebers, M., and Weber, M. (2007) Water balance of the highly
27 glaciated Vernagt Basin, Ötztal Alps. *Alpine space – Man & Environment*, 3.

- 1 Bronstert, A., Kolokotronis, V., Schwandt, D., Straub, H. (2007) Comparison and evaluation of
2 regional climate scenarios for hydrological impact analysis: general scheme and application
3 example. *Int. J. Clim.*, 27, 1579-1594.
- 4 Bronstert, A., Kneis, D., Bogena, H. (2009) Interaktionen und Rückkopplungen beim
5 hydrologischen Wandel: Relevanz und Möglichkeiten der Modellierung. *Hydrologie und*
6 *Wasserbewirtschaftung*, 53(5), 289-304.
- 7 Brunetti, M., Lentini, G., Maugeri, M., Nanni, T., Auer, I., Böhm, R., and Schöner, W. (2009)
8 Climate variability and change in the Greater Alpine Region over the last two centuries based on
9 multi-variable analysis. *Int. J. Climatol.*, 29, 2197-2225, doi:10.1002/joc.1857.
- 10 Cahynová, M. and Huth, R. (2009) Changes of atmospheric circulation in central Europe and
11 their influence on climatic trends in the Czech Republic. *Theor. Appl. Climatol.*, 96: 57–68, doi:
12 10.1007/s00704-008-0097-2.
- 13 Calcagno, V., and de Mazancourt, C. (2010) glmulti an R package for easy automated model
14 selection with (generalized) linear models. *J. Stat. Softw.*, 34, 1-29.
- 15 Dai, A., Qian, T., Trenberth, K., and Milliman, J. (2009) Changes in Continental Freshwater
16 Discharge from 1948 to 2004. *J. Climate*, 22, 2773–2792. doi: <http://dx.doi.org/10.1175/2008>
17 [JCLI2592.1](http://dx.doi.org/10.1175/2008)
- 18 Déry, S. J., Stahl, K., Moore, R. D., Whitfield, P. H., Menounos, B., and Burford, J. E. (2009)
19 Detection of runoff timing changes in pluvial, nival, and glacial rivers of western Canada. *Water*
20 *Resour. Res.*, 45, W04426, doi:10.1029/2008WR006975.
- 21 Déry, S. J., Stieglitz, M., McKenna, E. C., and Wood, E. F. (2005) Characteristics and trends of
22 river discharge into Hudson, James, and Ungava Bays, 1964 – 2000. *J. Clim.*, 18, 2540-2557.
- 23 Escher-Vetter, H., Braun, L., and Siebers, M. (2014) Hydrological and meteorological records
24 from the Vernagtferner Basin - Vernagtbach station, for the years 2002 to 2012.
25 doi:10.1594/PANGAEA.829530.
- 26 Gagnon, A. S., and Gough, W. A. (2002) Hydroclimatic trends in the Hudson bay region,
27 Canada. *Can. Water Resour. J.*, 27, 245-262, doi: 10.4296/cwrj2703245.

1 Garvelmann, J., Pohl, S., and Weiler, M. (2014) Spatio-temporal controls of snowmelt and
2 runoff generation during rain-on-snow events in a mid-latitude mountain catchment. *Hydrol.*
3 *Process.* (under review).

4 Hall, J., Arheimer, B., Borga, M., Brazdil, R., Claps, P., Kiss, A., Kjeldsen, TR, Kriaučiūnienė,
5 J., Kundzewicz, ZW, Lang, M., Llasat, MC., Macdonald, N., McIntyre, N., Mediero, L., Merz,
6 B., Merz, R., Molnar, P., Montanari, A., Neuhold, C., Parajka, J., Perdigão, R. A. P., Plavcová,
7 L., Rogger, M., Salinas, J. L., Sauquet, E., Schär, C., Szolgay, J., Viglione, A., and Blöschl, G.
8 (2013). Understanding flood regime changes in Europe: a state of the art assessment. *Hydrol.*
9 *Earth Syst. Sci.*, 18, 2735-2772.

10 Hall, A., Qu, X., and Neelin, J. D. (2008) Improving predictions of summer climate change in
11 the United States. *Geophys. Res. Lett.*, 35, L01702, doi:10.1029/2007GL032012.

12 Helsel, D.R., and Hirsch, R.M. (1992) *Statistical Methods in Water Resources*. Amsterdam:
13 Elsevier Science.

14 Jones, J. A. (2011) Hydrologic responses to climate change: considering geographic context and
15 alternative hypotheses. *Hydrological Processes*, 25(12), 1996-2000.

16 Kim, J.-S. & Jain, S. (2010) High-resolution streamflow trend analysis applicable to annual
17 decision calendars: A western United States case study. *Clim. Change*, 102 (3–4), 699–707.

18 Knowles, N., Dettinger, M. D., and Cayan, D. R. (2006) Trends in snowfall versus rainfall in the
19 Western United States. *J. Clim.*, 19, 4545-4559.

20 Kormann, C., Francke, T., and Bronstert, A. (2014) Detection of regional climate change effects
21 on alpine hydrology by daily resolution trend analysis in Tyrol, Austria, *J. Water Clim. Change*,
22 in press, doi: 10.2166/wcc.2014.099, 2014.

23 Livezey, R. E., and Chen, W. Y. (1983) Statistical Field Significance and its Determination by
24 Monte Carlo Techniques. *Mon. Wea. Rev.*, 111, 46-59. doi: 10.1175/1520-0493(1983)111
25 <0046:SFSaid>2.0. CO;2.

1 Magnusson, J., Jonas, T., Lopéz-Moreno, I. & Lehning, M. (2010) Snow cover response to
2 climate change in a high alpine and half-glacierized basin in Switzerland. *Hydrol. Res.* 41 (3–4),
3 230–240.

4 Merz, B., Maurer, T., and Kaiser, K. (2012a) Wie gut können wir vergangene und zukünftige
5 Veränderungen des Wasserhaushalts quantifizieren? *Hydrol. Wasserbewirtsch.*, 56 (5) 244-256.
6 doi: 10.5675/HyWa_2012,5_1.

7 Merz, B., Vorogushyn, S., Uhlemann, S., Delgado, J., Hundecha, Y., (2012b) HESS Opinions
8 "More efforts and scientific rigour are needed to attribute trends in flood time series", *Hydrol.*
9 *Earth Syst. Sci.*, 16, 1379-1387, doi: 10.5194/hess-16-1379-2012).

10 Mote, P. W., Hamlet, A. F., Clark, M. P., and Lettenmaier, D. P. (2005) Declining mountain
11 snowpack in Western North America. *B. Am. Meteorol. Soc.*, 39-49, doi:
12 10.1175/BAMS-86-1-39.

13 Morin, E. (2011) To know what we cannot know: Global mapping of minimal detectable
14 absolute trends in annual precipitation. *Water Resour. Res.*, 47, W07505,
15 doi:10.1029/2010WR009798.

16 Nemec J., Gruber, G., Chimani, B., and Auer, I. (2012) Trends in extreme temperature indices in
17 Austria based on a new homogenized dataset. *Int. J. Climatol.*, doi: 10.1002/joc.3532.

18 Neudorfer, T., Pinter, M., Kimer, L., Wendter, S., and Messner, W. (2012) Milchwirtschaft auf
19 Österreichs Almen - Entwicklungen und wirtschaftliche Perspektiven. BMLFUW, Vienna.

20 Parajka, J., Kohnová, S., Merz, R., Szolgay, J., Hlavčová, K., Blöschl, G. (2009) Comparative
21 analysis of the seasonality of hydrological characteristics in Slovakia and Austria, *Hydrol. Sci. J.*,
22 54, 456-473, doi: 10.1623/hysj.54.3.456

23 Parajka, J., Kohnová, S., Bálint, G., Barbuc, M., Borga, M., Claps, P., Cheval, S., Dumitrescu,
24 A., Gaume, E., Hlavčová, K., Merz, R., Pfaundler, M., Stancalie, G., Szolgay, J., and Blöschl, G.
25 (2010) Seasonal characteristics of flood regimes across the Alpine–Carpathian range. *J. Hydrol.*,
26 394(1), 78-89.

1 Parry, M.L., Canziani, O.F., Palutikof, J.P., van der Linden, P.J., and Hanson, C.E. (Ed.) (2007)
2 *Climate Change 2007: Impacts, Adaptation and Vulnerability*. Contribution of Working Group II
3 to the Fourth Assessment Report of the Intergovernmental Panel on Climate Change. Cambridge:
4 Cambridge University Press.

5 Paterson, W.S.B. (1994) *The physics of glaciers* (third edition). Oxford: Pergamon Press, 480 pp.

6 Pellicciotti, F., Bauder, A., and Parola, M. (2010) Effect of glaciers on streamflow trends in the
7 Swiss Alps. *Water Resour. Res.*, 46, W10522, doi:10.1029/2009WR009039.

8 Pekarova, P., Miklanek, P., and Pekar, J. (2006) Long-term trends and runoff fluctuations of
9 European rivers. In *Climate Variability and Change - Hydrological Impacts*, IAHS: UK;
10 520-525.

11 Renner, M., and Bernhofer, C. (2011) Long term variability of the annual hydrological regime
12 and sensitivity to temperature phase shifts in Saxony/Germany, *Hydrol. Earth Syst. Sci.*, 15,
13 1819-1833, doi:10.5194/hess-15-1819- 2011.

14 Scherrer, S. C., Appenzeller, C. and Laternser, M. (2004) Trends in Swiss Alpine snow days:
15 The role of local- and large-scale climate variability, *Geophys. Res. Lett.*, 31, L13215,
16 doi:10.1029/2004GL020255.

17 Schimon, W., Schöner, W., Böhm, R., Haslinger, K., Blöschl, G., Merz, R., Blaschke, A. P.,
18 Viglione, A., Parajka, J., Kroiß, H., Kreuzinger N., and Hörhan, T. (2011) Anpassungsstrategien
19 an den Klimawandel für Österreichs Wasserwirtschaft. Bundesministerium für Land- und
20 Forstwirtschaft, Umwelt und Wasserwirtschaft, Vienna, Austria.

21 Stahl, K., and Moore, R. D. (2006) Influence of watershed glacier coverage on summer
22 streamflow in British Columbia, Canada. *Water Resour. Res.*, 42, W06201,
23 doi:10.1029/2006WR005022.

24 Stahl, K., Hisdal, H., Hannaford, J., Tallaksen, L. M., van Lanen, H. A. J., Sauquet, E., Demuth,
25 S., Fendekova, M., and Jódar, J. (2010) Streamflow trends in Europe: evidence from a dataset of
26 near-natural catchments, *Hydrol. Earth Syst. Sci.*, 14, 2367-2382, doi:10.5194/hess-14-2367-
27 2010.

- 1 Stewart, I., Cayan, D., and Dettinger, M. (2005) Changes toward earlier streamflow timing
2 across western North America. *J. Climate*, 18, 1136-1155.
- 3 Stine, A., Huybers, P., and Fung, I. (2009) Changes in the phase of the annual cycle of surface
4 temperature. *Nature*, 457, 435-440.
- 5 Tecklenburg, C., Francke, T., Kormann, C. & Bronstert, A. (2012) Modeling of water balance
6 response to an extreme future scenario in the Ötztal catchment, Austria. *Adv. Geosci.*, 32, 63–68.
- 7 Viviroli, D., Archer, D.R., Buytaert, W., Fowler, H.J., Greenwood, G.B., Hamlet, A.F., Huang,
8 Y., Koboltschnig, G., Litaor, I., López-Moreno, J.I., Lorentz, S., Schädler, B., Schreier, H.,
9 Schwaiger, K., Vuille, M., and Woods, R. (2011) Climate Change and Mountain Water
10 Resources: Overview and Recommendations for Research, Management and Policy. *Hydrol.*
11 *Earth Syst. Sci.*, 15, 471–504. doi:10.5194/hess-15-471-2011.
- 12 Vormoor, K., Lawrence, D., Heistermann, M., and Bronstert, A. (2014) Climate change impacts
13 on the seasonality and generation processes of floods in catchments with mixed
14 snowmelt/rainfall regimes: projections and uncertainties, *Hydrol. Earth Syst. Sci. Discuss.*, 11,
15 6273-6309, doi:10.5194/hessd-11-6273-2014,.
- 16 Walter, M. T., Wilks, D. S., Parlange, J. and Schneider, R. L. (2004) Increasing
17 evapotranspiration from the conterminous United States. *J. Hydrometeorol.*, 5 (3), 406-408.
- 18 Walther G.-R. (2003) Plants in a warmer world. *Perspect. Plant Ecol. Evol. Syst.*, 6, 169-185.
- 19 Weber, M., Prasch, M., Kuhn, M., Lambrecht, A. and Hagg, W. (2009) Ice reserves – sub-project
20 glaciology, Chapter 1.8, GLOWA-Danube-Project, LMU Munich: Global Change Atlas,
21 Munich.
- 22 Weber, M., Braun, L., Mauser, W., and Prasch, M. (2010) Contribution of rain, snow- and
23 icemelt in the upper danube discharge today and in the future. *Geogr. Fis. Dinam. Quat.*, 33,
24 221-230.
- 25 Whitfield, P. H. (2013) Is ‘Centre of Volume’ a robust indicator of changes in snowmelt timing?
26 *Hydrol. Process.*, 27, 2691-2698. doi: 10.1002/hyp.9817.

1 Yue, S., and Wang, C. Y. (2002) Applicability of prewhitening to eliminate the influence of
2 serial correlation on the Mann-Kendall test. *Water Resour. Res.*, 38 (6), 1068,
3 doi:10.1029/2001WR000861.

4

1 Appendix

2 A.1 Schematic illustration on the structure of the analyses

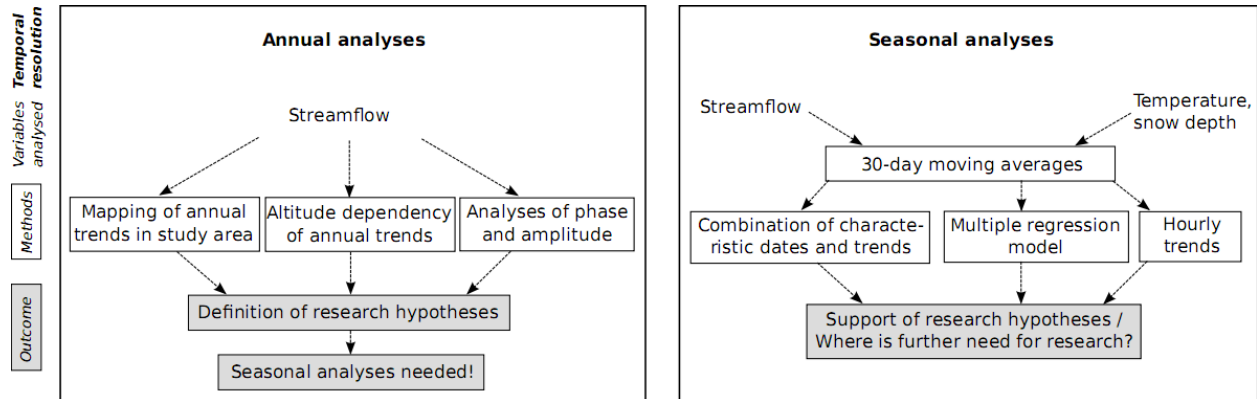


Figure A.1: Schematic illustration on the structure of the analyses.

5 A.2 List of symbols and abbreviations

Symbol	Unit	Property
α	-	significance level
α_{local}	-	local significance level
α_{field}	-	field significance level
Δ	var. units/year	trend
ΔQ_{year}	mm/year	trend of annual Q means
ΔQ_{30DMA}	mm/year	trend of $30DMA$ Q means, for certain DOY at certain station
$\overline{\Delta T_{\text{min}}}$	°C per year	mean trend in T_{min} , averaged over all stations, for certain DOY
Δ_{MD}	var. units/year	minimal detectable trend
σ_X	variable units	standard deviation
$30DMA$	variable units	30-day moving averages
$A_{\text{ice}}/A_{\text{tot}}$	%	Percentage of glaciated area in the watershed
DOY	-	day of year

\overline{DOY}	-	characteristic date (average <i>DOY</i> of a certain event)
$\overline{DOY}_{0^\circ T_{meanSpring}}$	-	average <i>DOY</i> , when T_{mean} crosses 0 °C in spring (1980-2010)
$\overline{DOY}_{Q_{max}}$	-	average <i>DOY</i> , when annual <i>Q</i> maximum occurs (1980-2010)
$\overline{DOY}_{SD_{max}}$	-	average <i>DOY</i> , when annual <i>SD</i> maximum occurs (1980-2010)
<i>ET</i>	mm	evapotranspiration
<i>Q</i>	mm	specific runoff
Q_{year}	mm	annual <i>Q</i> mean
Q_{30DMA}	mm	<i>30DMA Q</i> for certain <i>DOY</i>
\overline{Q}_{30DMA}	mm	<i>30DMA Q</i> , averaged for 1980-2010, for certain <i>DOY</i>
\dot{Q}_{30DMA}	mm	first derivative of \overline{Q}_{30DMA}
<i>SD</i>	cm	snow depths
<i>S/N</i>	-	signal-to-noise ratio
T_{max}	°C	daily maximum temperature
T_{mean}	°C	daily mean temperature
T_{min}	°C	daily minimum temperature
<i>R</i>	-	record length

Table 1: List of the gauging stations used in this study (sorted by mean altitude) and their characteristics.

Station ID	Station name (and ID of nested basin)	Altitude (m)	Latitude	Longitude	Gauged Area (km ²)	Mean basin alt. (m)	Glacier coverage (%)
1	<i>Vernagt</i>	2640	46.8678	10.8007	11	3127	71.9
2	<i>Vent</i> (1)	1891	46.8665	10.8895	90	2934	33.0
3	<i>Gepatschalm</i>	1895	46.9112	10.7142	55	2880	39.3
4	<i>Obergurgl</i>	1883	46.8717	10.9998	73	2849	28.2
5	<i>Huben</i> (1, 2, 4)	1186	47.0508	10.9598	517	2700	15.7
6	<i>St. Leonhard</i>	1337	47.0796	10.8312	167	2613	15.5
7	<i>Hinterbichl</i>	1321	47.0026	12.3380	107	2600	14.3
8	<i>Innergschlöß</i>	1687	47.1099	12.4551	39	2590	29.4
9	<i>Tumpen</i> (1, 2, 4, 5)	924	47.1707	10.9031	786	2579	11.8
10	<i>Ritzenried</i> (6)	1095	47.1329	10.7711	220	2544	13.2
11	<i>Neukaser</i>	1824	47.0225	11.6877	24	2499	9.6
12	<i>Tauernhaus</i> (8)	1504	47.1037	12.4990	60	2474	19.4
13	<i>Spöttling</i>	1486	47.0106	12.6358	47	2473	10.6
14	<i>Kühtai</i>	1902	47.2124	10.9994	9	2448	0.0
15	<i>Galtür-Au</i>	1544	46.9988	10.1747	98	2411	5.7
16	<i>Waier</i> (7)	931	46.9798	12.5290	285	2376	8.4
17	<i>Sulzau</i>	882	47.2185	12.2508	81	2354	17.2
18	<i>Fundusalm</i>	1600	47.1492	10.8909	13	2336	0.0
19	<i>See i. P.</i>	1019	47.1051	10.4541	385	2303	1.6
20	<i>Habach</i>	880	47.2322	12.3276	45	2117	6.9
21	<i>Mallnitz</i>	1174	46.9661	13.1835	85	2081	0.6
22	<i>Steeg</i>	1113	47.2643	10.2867	248	1951	0.0
23	<i>Bad Hofgastein</i>	837	47.1456	13.1184	221	1937	1.3
24	<i>Haidbach</i>	888	47.2377	12.4921	75	1915	0.0
25	<i>Rauris</i>	917	47.2233	12.9999	242	1841	1.6
26	<i>Vorderhornbach</i> (22)	958	47.3842	10.5389	64	1726	0.0
27	<i>Hopfreben</i>	943	47.3144	10.0416	42	1701	0.0
28	<i>Wagrain</i>	849	47.3102	13.3112	91	1594	0.0
29	<i>Viehhofen</i>	861	47.3487	12.7448	151	1550	0.0
30	<i>Mellau</i> (27)	673	47.3881	9.8790	229	1494	0.0
31	<i>Laterns</i>	830	47.2956	9.7195	33	1475	0.0
32	<i>Ehrwald</i>	958	47.4150	10.9159	88	1467	0.0

Table 2: Pearson's r between annual streamflow trends and mean watershed altitude.

	Significant trends only	Insignificant trends only	Both
$\Delta Q_{\overline{year}}$, percent	0.84	0.54	0.68
$\Delta Q_{\overline{year}}$, absolute	0.81	0.65	0.62
$\Delta Q_{\overline{phase}}$	0.86	0.68	0.83
$\Delta Q_{\overline{amplitude}}$	0.87	0.74	0.76

Fig. 1: Study area with meteorological stations, watershed boundaries, glaciers and trends of mean annual streamflow in percent change per year (period: 1980–2010; significance level: $\alpha=0.1$). Station ID next to the triangles.

Fig. 2: Trend magnitude (percent and absolute values, resp.) versus station ID (sorted by rank of mean watershed altitude (1 = highest)).

Fig. 3: Seasonal distribution of daily streamflow trends (period: 1980–2010; significance level: $\alpha=0.1$); **a)** 30DMA trend magnitude, only where significant trends are detected (dark blue if not significant); **b)** 30DMA trend magnitude, without assigning significance; white squares: average annual Q maxima; bar above upper diagram: pink-coloured if the 30-DMA trends are field-significant; bar on the right of upper diagram: pink-coloured if the *annual* streamflow trend of the corresponding station is significant.

Fig. 4: **a)** Station altitude vs. \overline{DOY} of daily T_{mean} passing the freezing point in spring; **b)** same as **a)**, but for autumn; **c)** station altitude vs. \overline{DOY} of annual SD maximum; all graphs with the line of best fit and corresponding equation. DOYs are calculated as averages of the period 1980–2010.

Fig. 5: **a) - d)** Seasonal distribution of daily mean (a), minimum (b) and maximum (c) temperature, (d) snow depth trend magnitudes and e) streamflow trends (with characteristic dates) (1980–2010); bar above diagram: black-coloured if field significant.

Fig. 6: Scatterplot of predicted vs. observed streamflow trends in percent per year on the day considered.

Fig. 7: Seasonal distribution of hourly trend magnitudes (1985–2010); a) T at Vernagt; b) Q at Gepatschalm; c) Q at Obergurgl; d) Q at Tumpen.

Fig. 8: Long-term annual streamflow cycle of a) a higher-altitude watershed (Gepatschalm, 2880 m, 39.3 % glaciated), b) a mid-altitude, little glaciated watershed (See i. P., 2303 m, 1.6 % glaciated) and c) a lower-altitude, unglaciated watershed (Ehrwald, 1467 m), trends generated from the end point of the Sen's Slope Estimator (dashed line, similar to Déry et al., 2009) and potential causes. Long arrows correspond to strong drivers, short arrows to smaller ones.

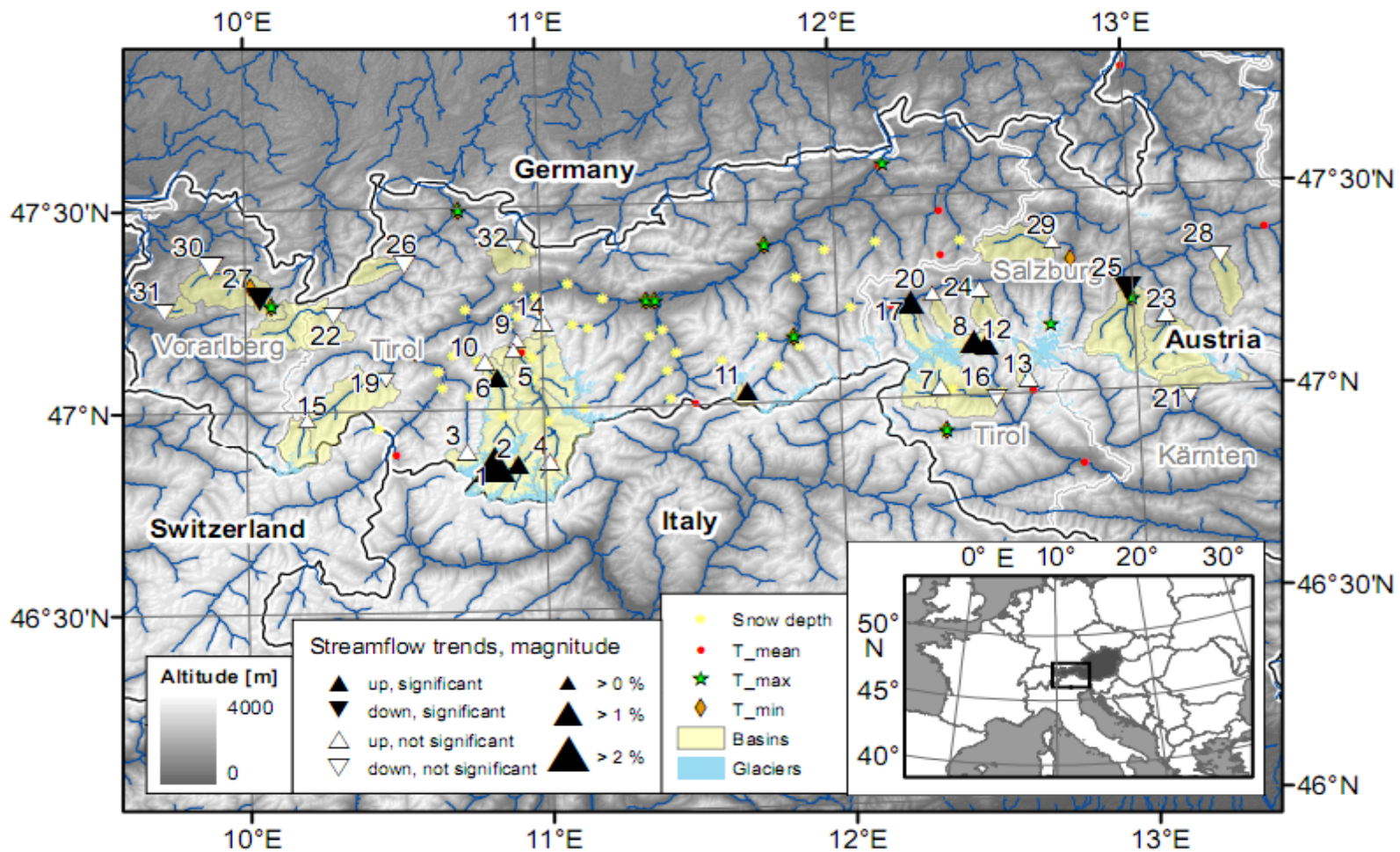


Fig. 1

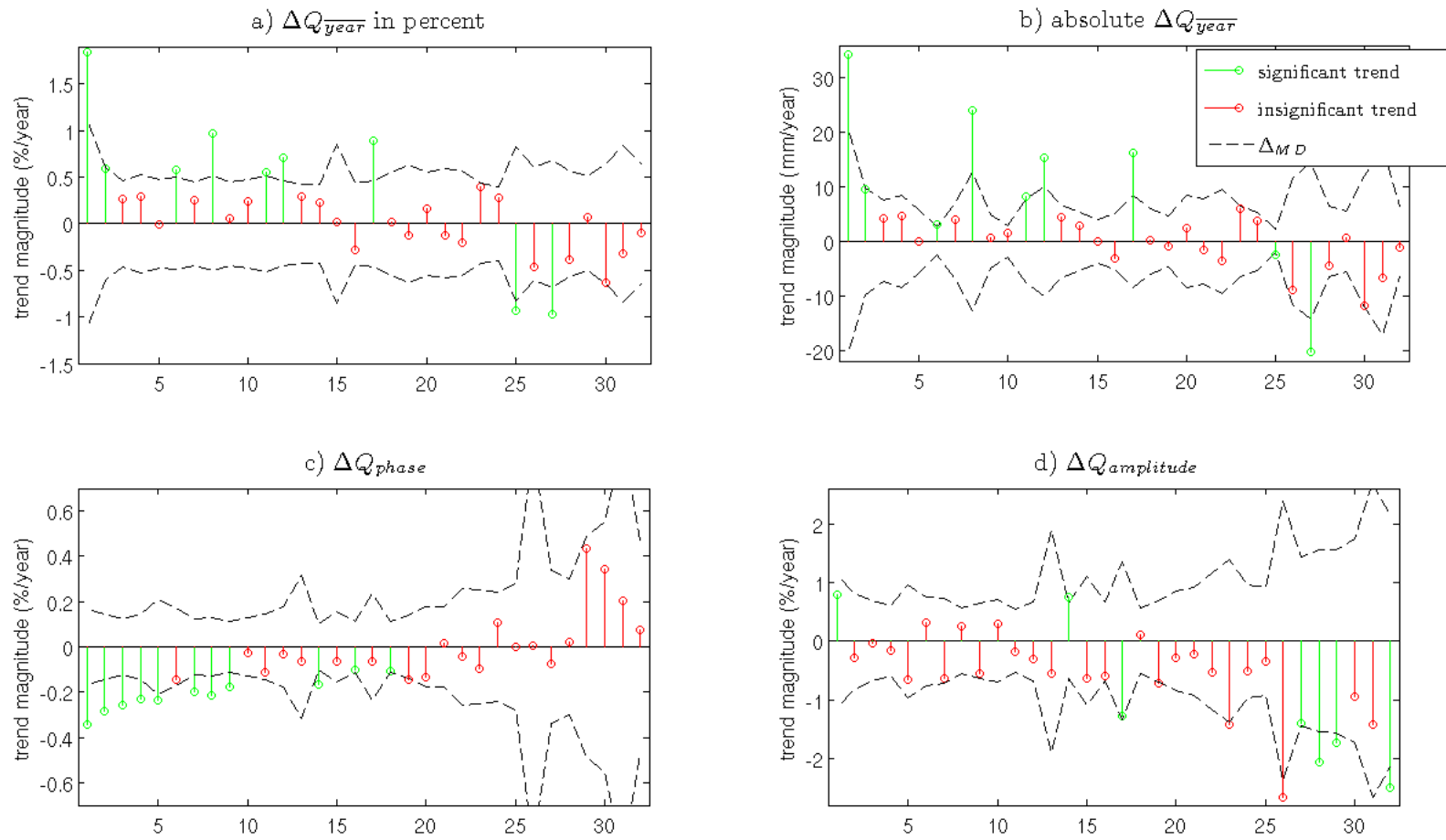


Fig. 2

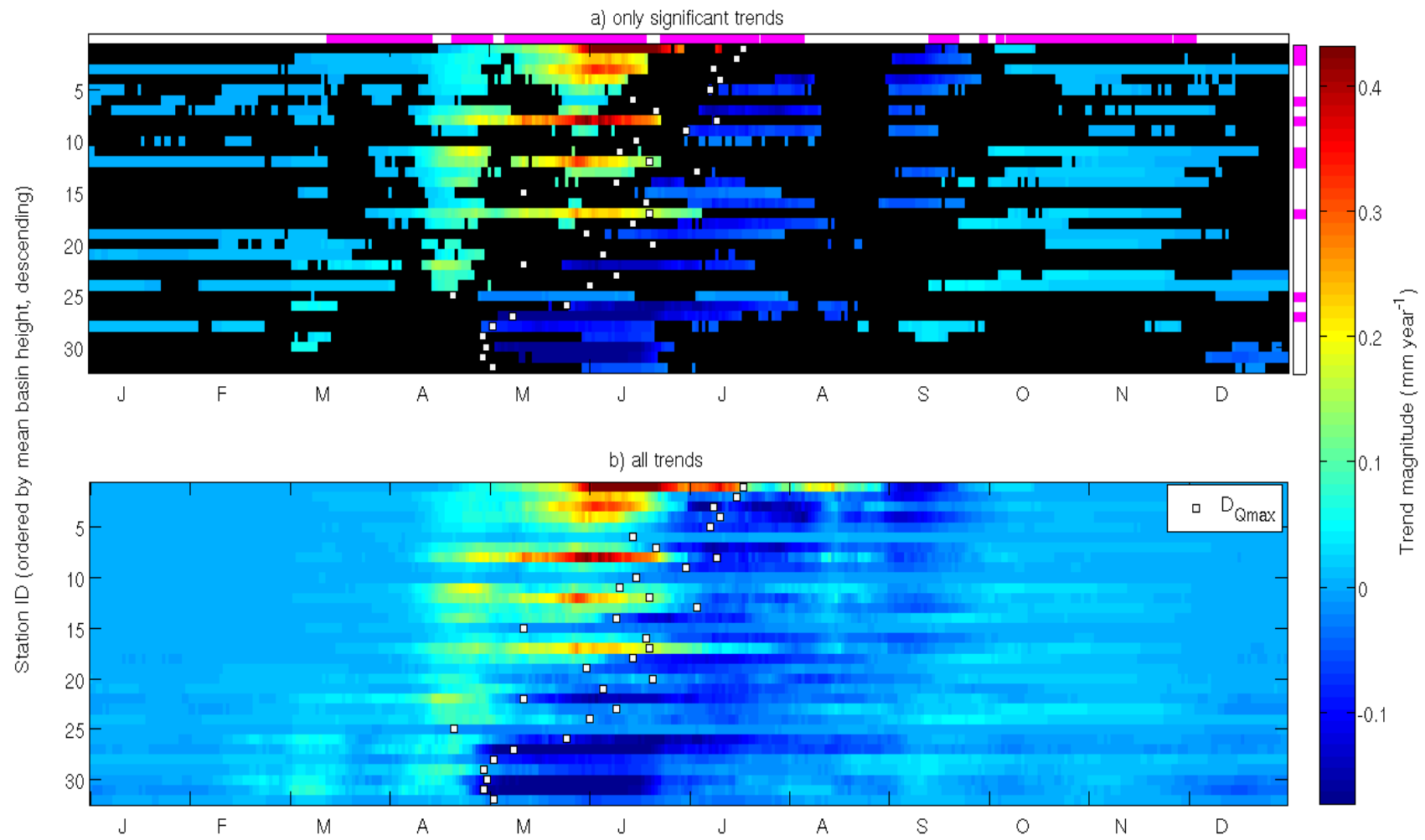


Fig. 3

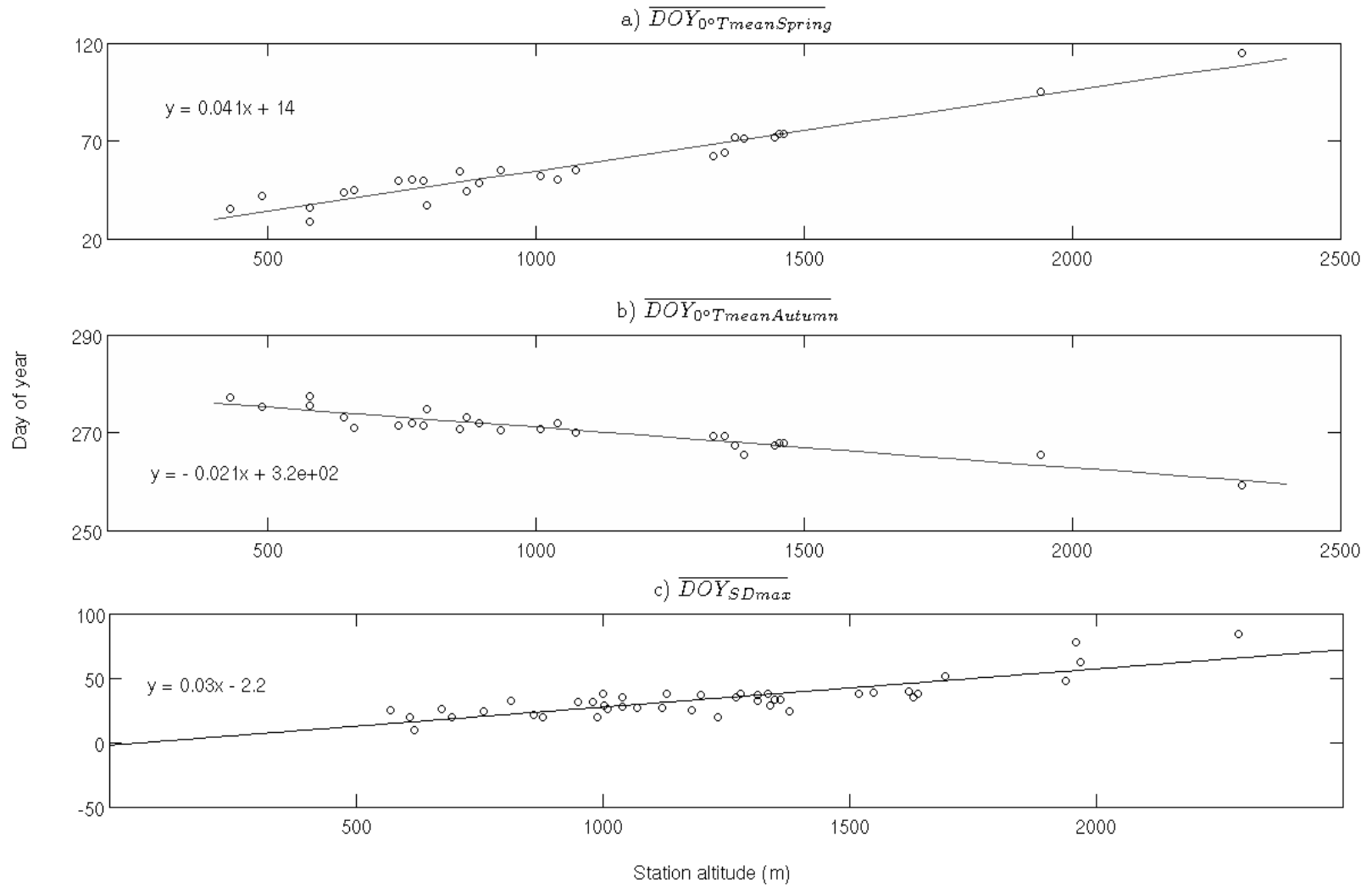


Fig. 4

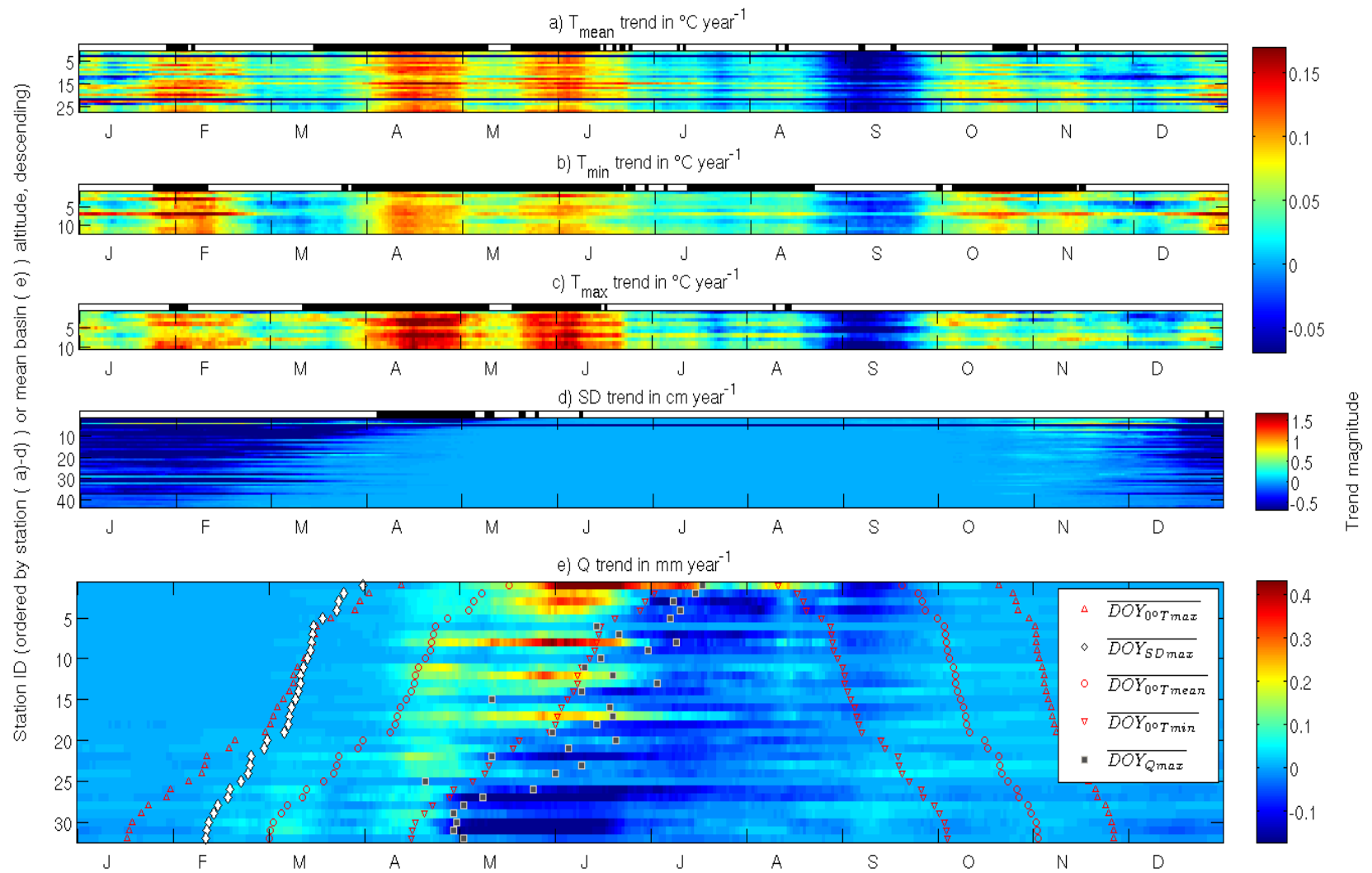


Fig. 5

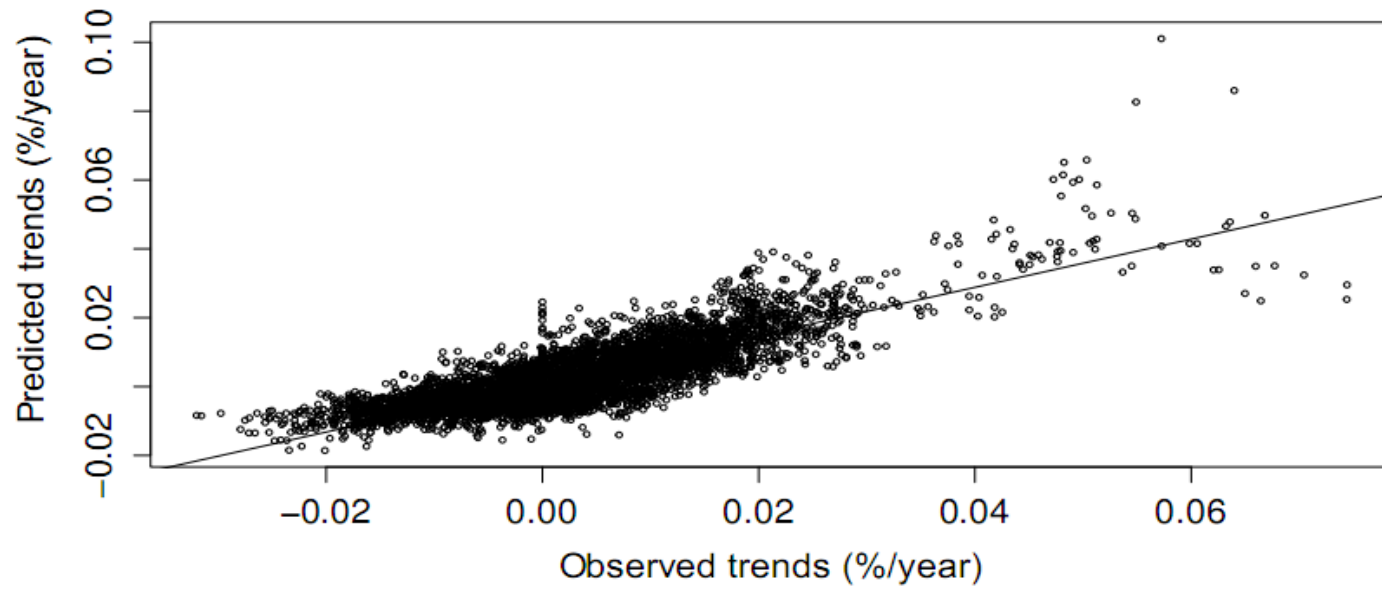


Fig. 6

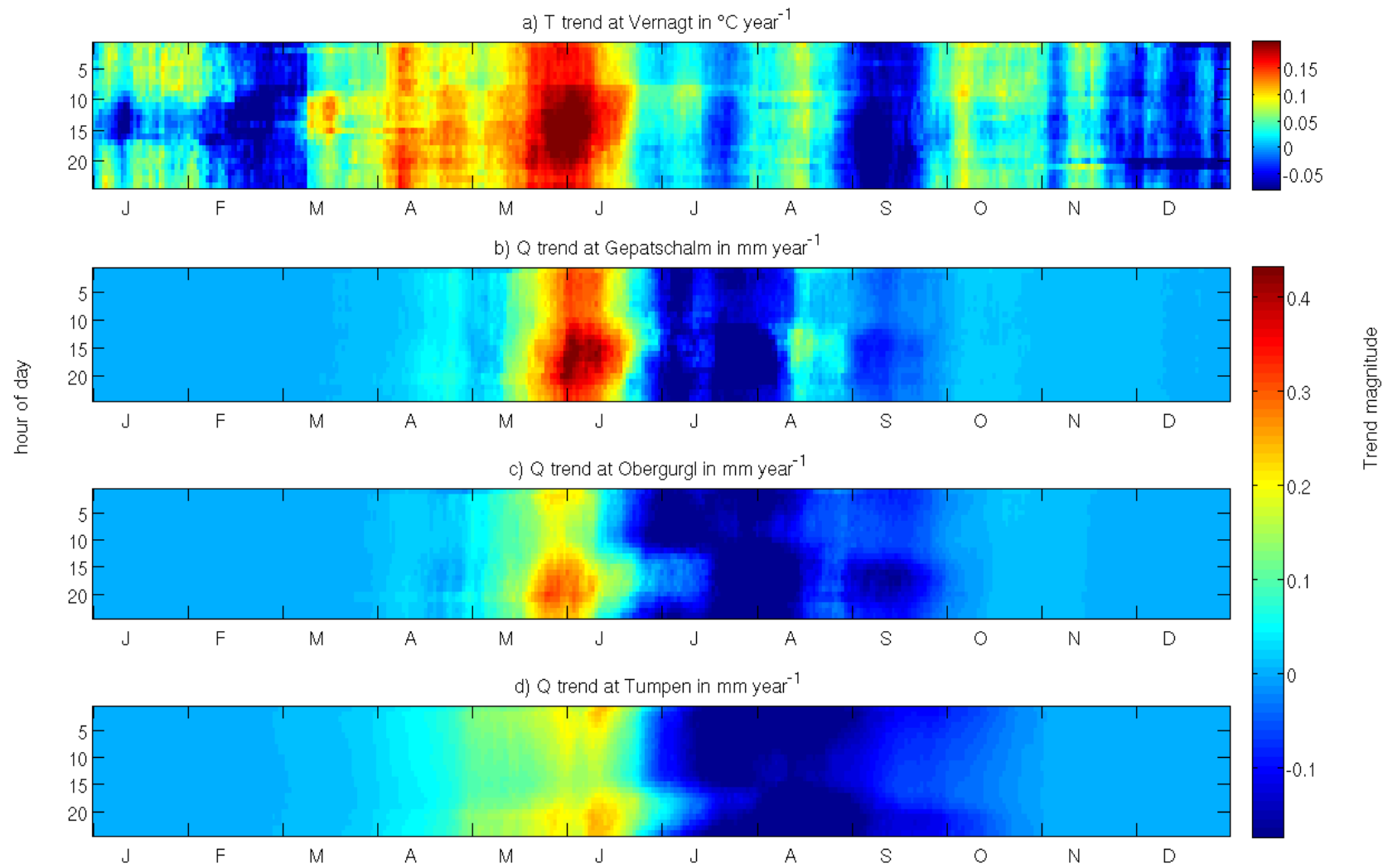


Fig. 7

Fig. 8

